Thermal Conduction in High-Beta Turbulent Plasma

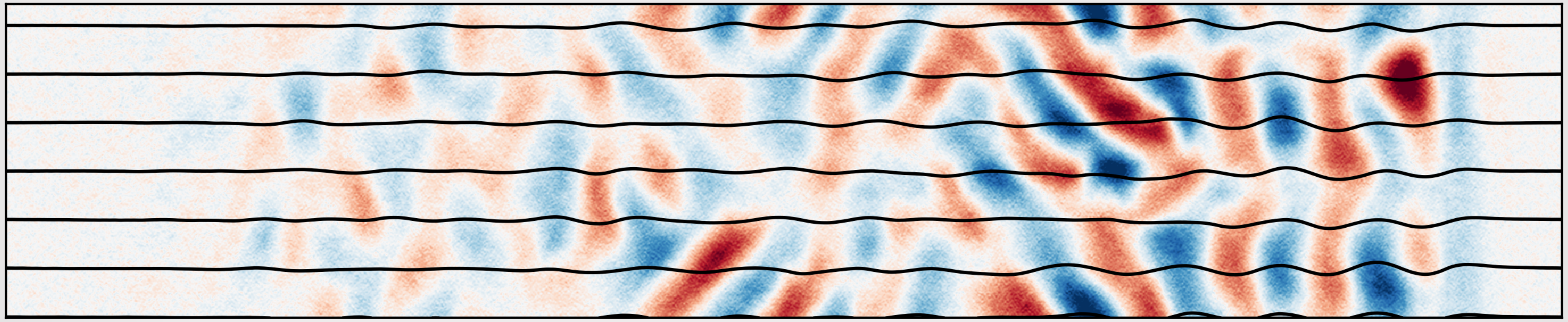

S. Komarov (Cambridge), E. Churazov (MPA),
A. Schekochihin (Oxford), M. Kunz (Princeton),
A. Spitkovsky (Princeton)

Outline

- Thermal conduction in weakly collisional plasmas
- Suppression mechanisms
  - Local suppression by turbulence
  - Mirror instability
  - Whistler instability
- Summary

Weakly collisional plasmas

galaxy clusters, accretion disks, (solar wind):

$$L \gtrsim \lambda_{\mathrm{mfp}} \gg \rho_i$$

$\Downarrow$ + turbulence

anisotropic pressure,
anisotropic particle transport,
Larmor-scale instabilities $\Rightarrow$

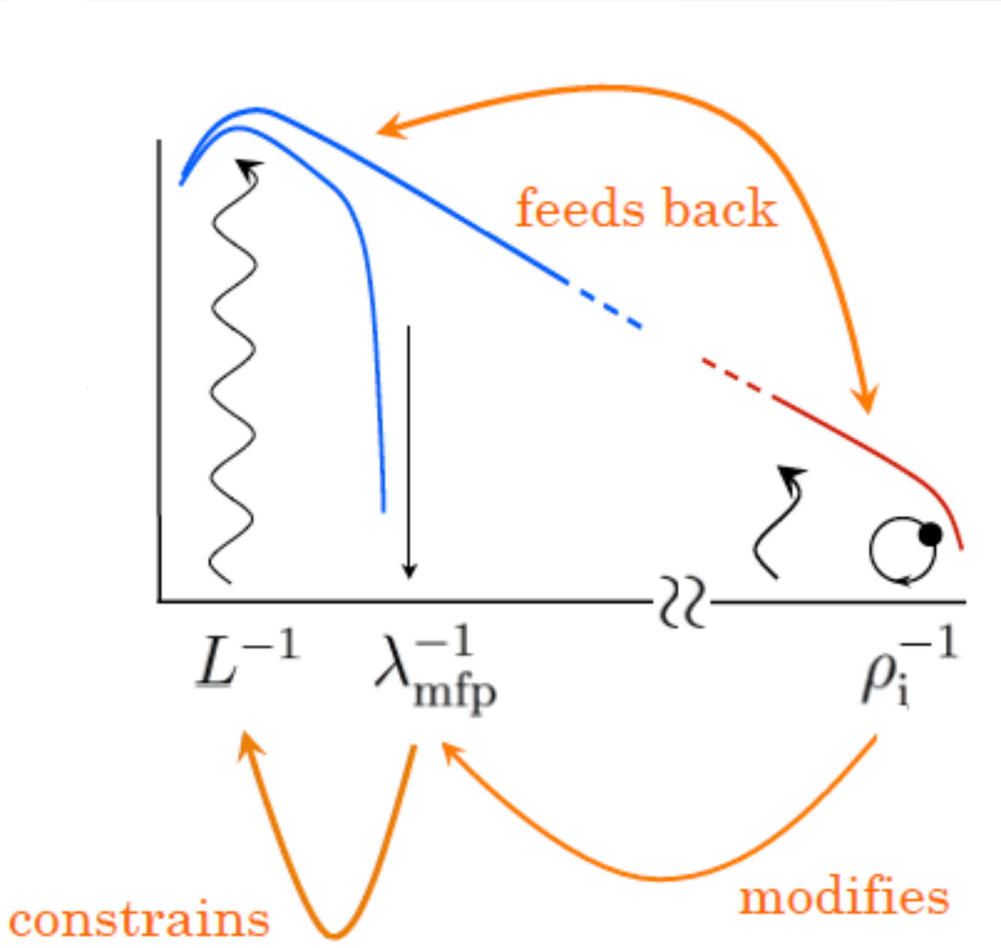

Matt's sketch

Weakly collisional plasmas

galaxy clusters, accretion disks, (solar wind):

$$L \gtrsim \lambda_{\mathrm{mfp}} \gg \rho_i$$

$\Downarrow$ + turbulence

anisotropic pressure,
anisotropic particle transport,
Larmor-scale instabilities $\Rightarrow$

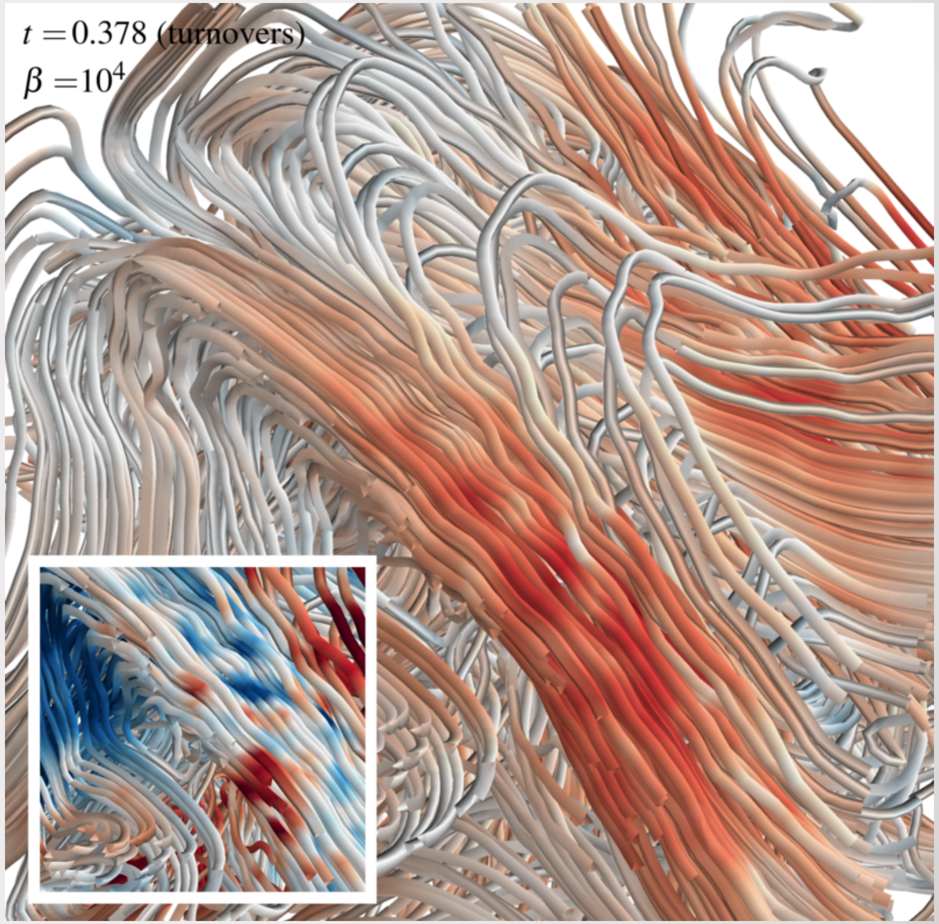

Rincon et al. 2016

thermal conduction in such system?

Temperature variations in galaxy clusters

A520 temperature map
Wang et al. 2016

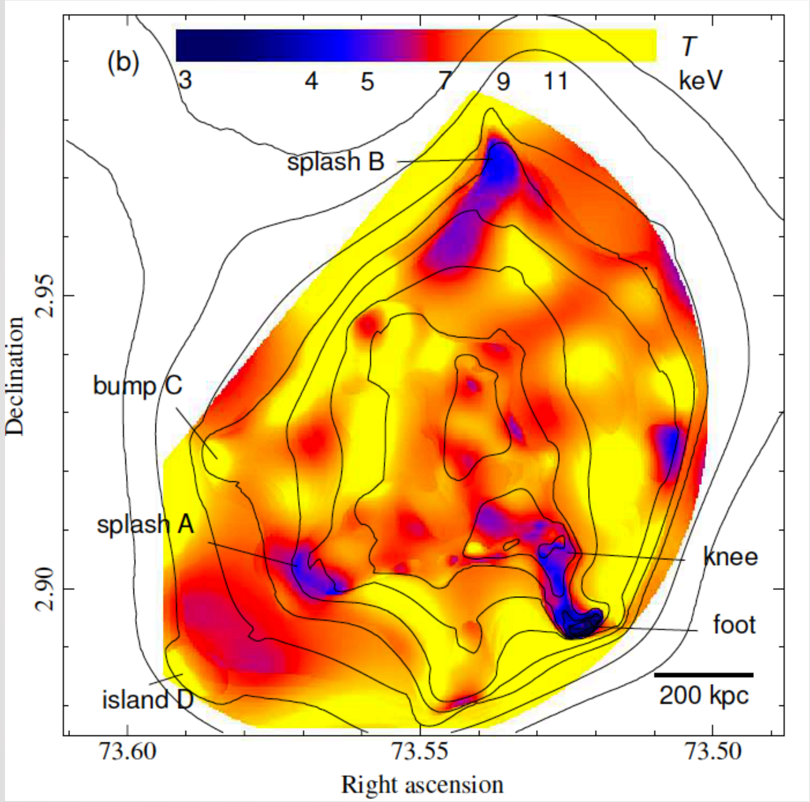

$$\tau_{cond} \sim n_e k_B l_T^{\ 2} / \kappa_{Sp} \approx 10^7\, yr \left(\frac{l_T}{100kpc} \right)^2$$

n ~ 10^{-3} cm^{-3} B ~ 1-10 μG
T ~ 1-10 keV $\beta \sim 100$
$\lambda_{mfp} \sim 10$ kpc $\rho_e \sim$ npc

Fang et al. 2018

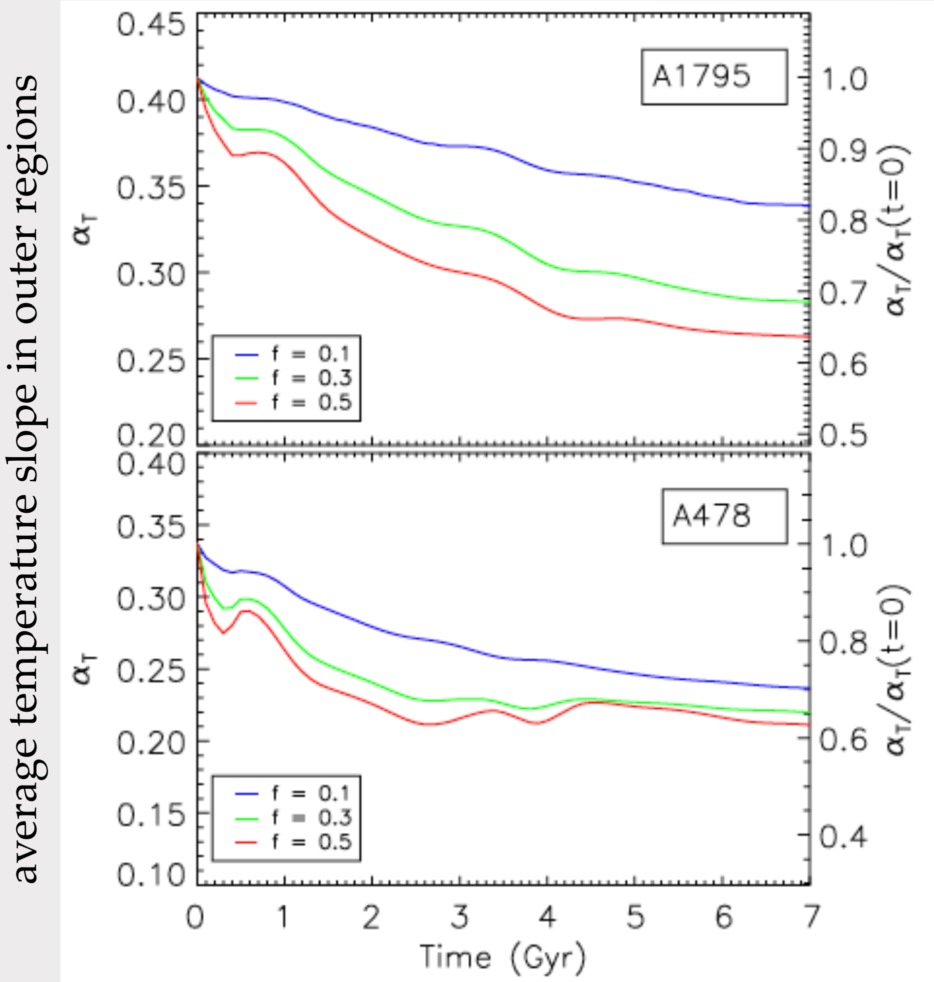

observed temperature profiles in outer regions are similar => suppression factor ≲0.1 for radial magnetic field

Heat flux inhibition in solar wind

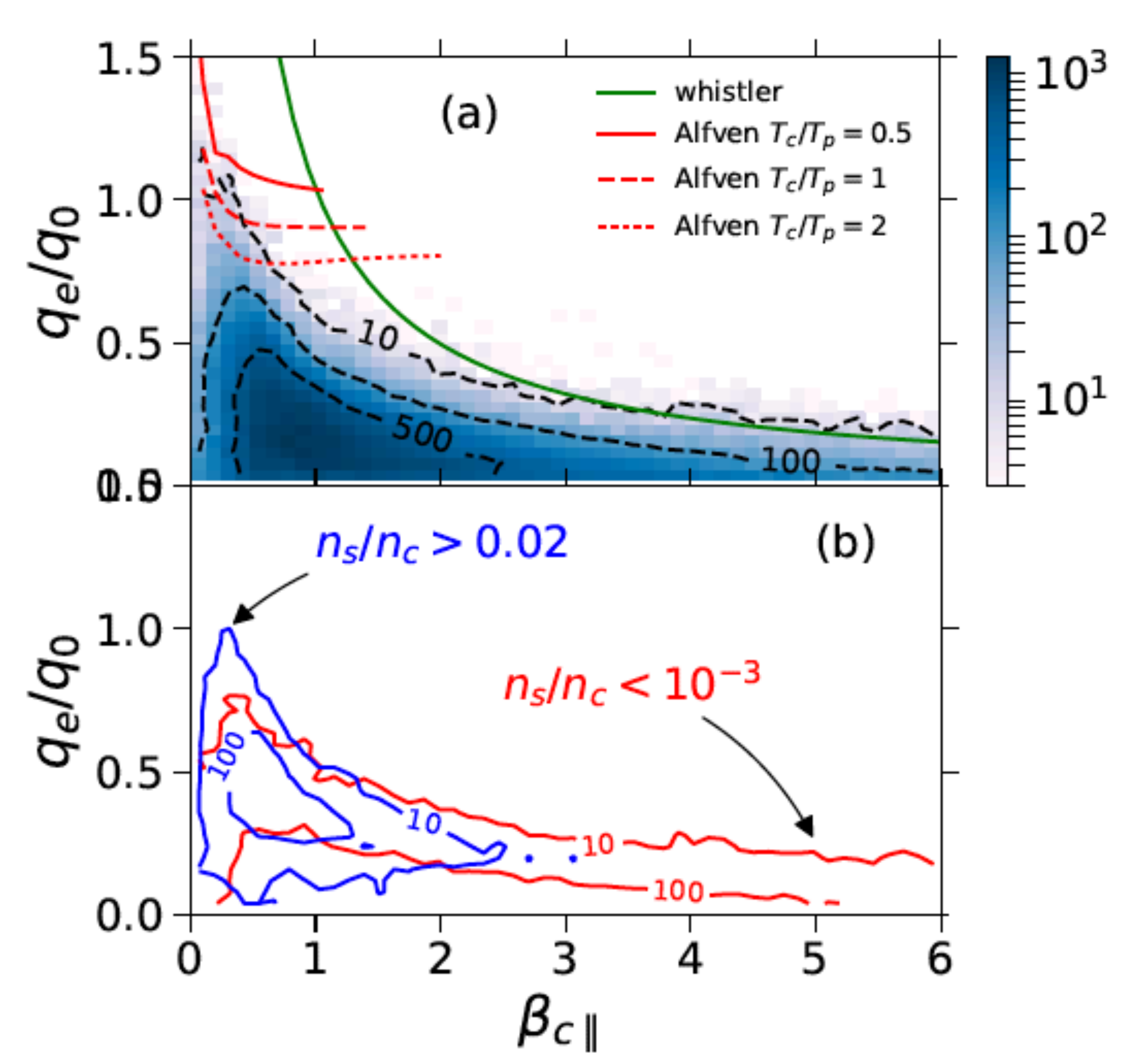

Tong+ 2018

Mechanisms of heat-flux suppression

From radio observations ρ_e/λ_{mfp}~10^{-13} --> heat conduction along field lines

Mechanisms of heat-flux suppression

From radio observations ρ_e/λ_{mfp}~10^{-13} --> heat conduction along field lines

- Cluster scale: field is tangled by turbulence.
  Suppression S~1/5-1/3 (Narayan & Medvedev 2001).

Mechanisms of heat-flux suppression

From radio observations ρ_e/λ_{mfp}~10^{-13} --> heat conduction along field lines

- Cluster scale: field is tangled by turbulence.
  Suppression S~1/5-1/3 (Narayan & Medvedev 2001).

- Scale of turbulent/ordered motions : $B \perp \nabla T$.
  Komarov+ 2014

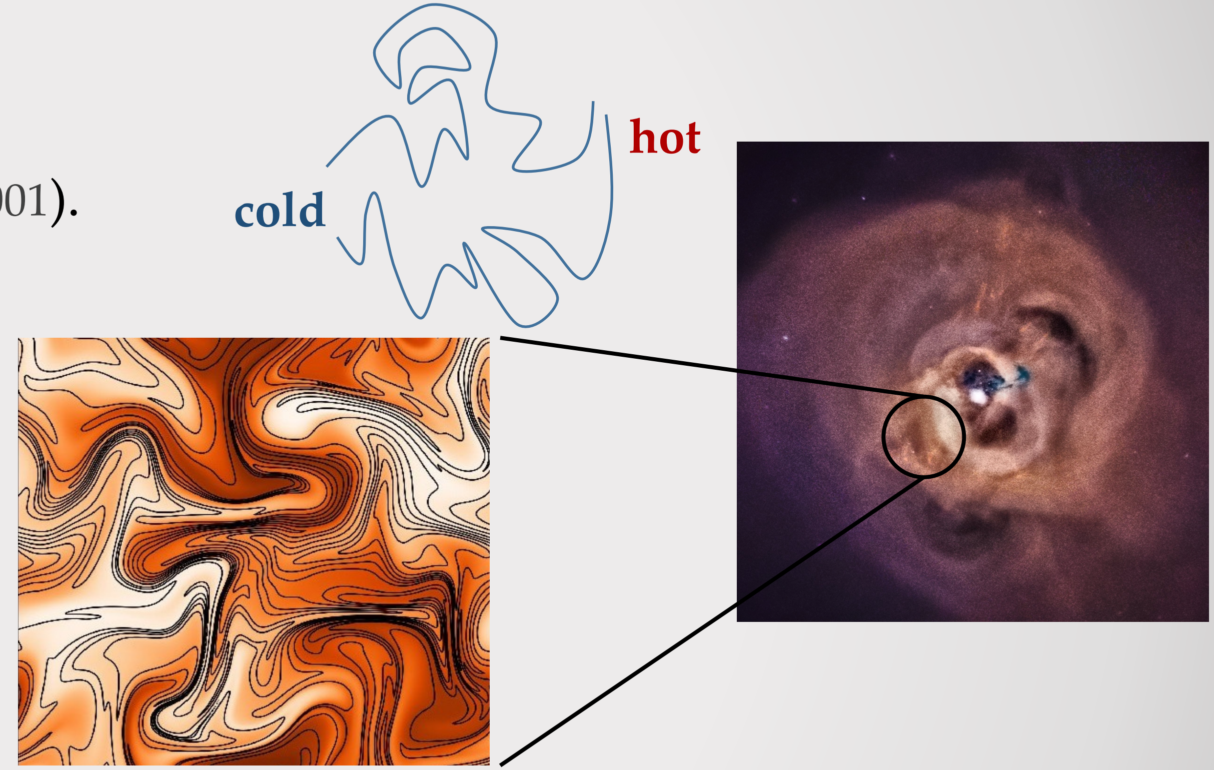

Mechanisms of heat-flux suppression

From radio observations $\rho_e/\lambda_{mfp} \sim 10^{-13}$ --> heat conduction along field lines

- Cluster scale: field is tangled by turbulence.
  Suppression S~1/5-1/3 (Narayan & Medvedev 2001).

- Scale of turbulent/ordered motions : $B \perp \nabla T$.
  Komarov+ 2014

- Scales $\ll L_B$: plasma instabilities
  Pressure anisotropy->
  ion mirror instability, S~1/5
  Komarov+ 2016

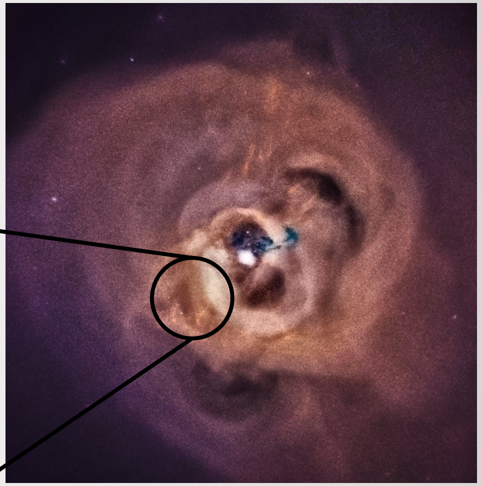

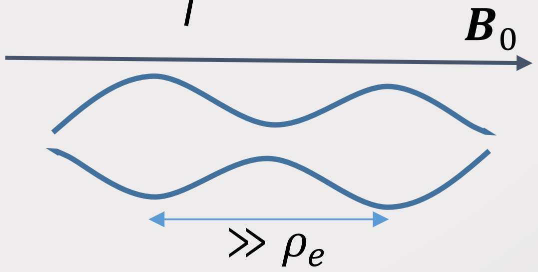

Mechanisms of heat-flux suppression

From radio observations ρ_e/λ_{mfp}~10^{-13} --> heat conduction along field lines

- Cluster scale: field is tangled by turbulence.
  Suppression S~1/5-1/3 (Narayan & Medvedev 2001).
- Scale of turbulent/ordered motions : $B \perp \nabla T$.
  Komarov+ 2014
- Scales $\ll L_B$: plasma instabilities
  Pressure anisotropy->
  ion mirror instability, S~1/5
  Komarov+ 2016

Weakly collisional heat flux ->
electron whistler instability

Gary+ 1975, Levinson & Eichler 1992, Pistinner 1998,
Roberg-Clark+ 2018, Komarov+ 2018

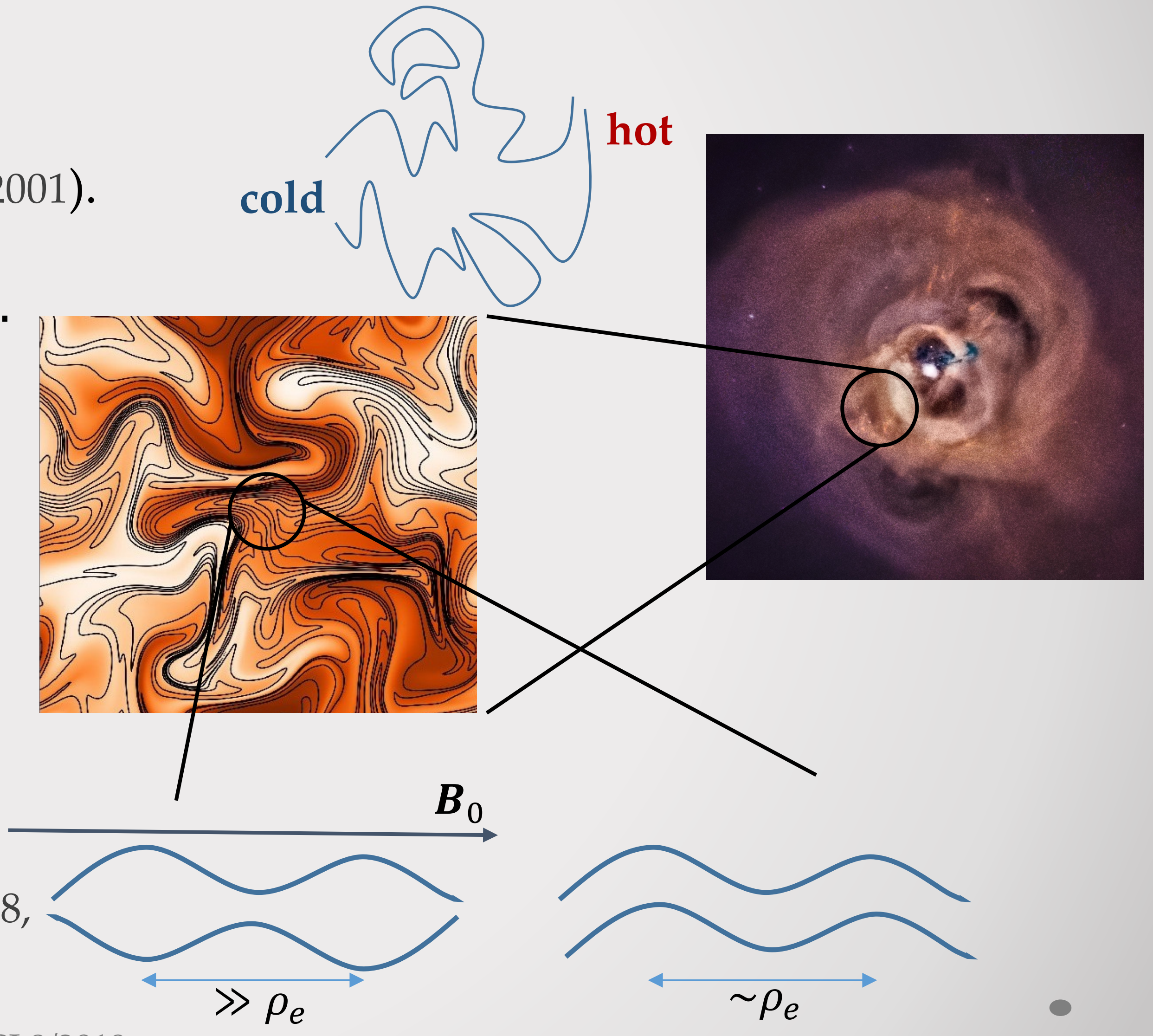

Mechanisms of heat-flux suppression

From radio observations $\rho_e/\lambda_{mfp} \sim 10^{-13}$ --> heat conduction along field lines

- Cluster scale: field is tangled by turbulence.
  Suppression S~1/5-1/3 (Narayan & Medvedev 2001).

- <u>Scale of turbulent/ordered motions</u> : $B \perp \nabla T$.
  Komarov+ 2014

- Scales $\ll L_B$: plasma instabilities
  Pressure anisotropy->
  ion mirror instability, S~1/5
  Komarov+ 2016

Weakly collisional heat flux ->
electron whistler instability

Gary+ 1975, Levinson & Eichler 1992, Pistinner 1998,
Roberg-Clark+ 2018, Komarov+ 2018

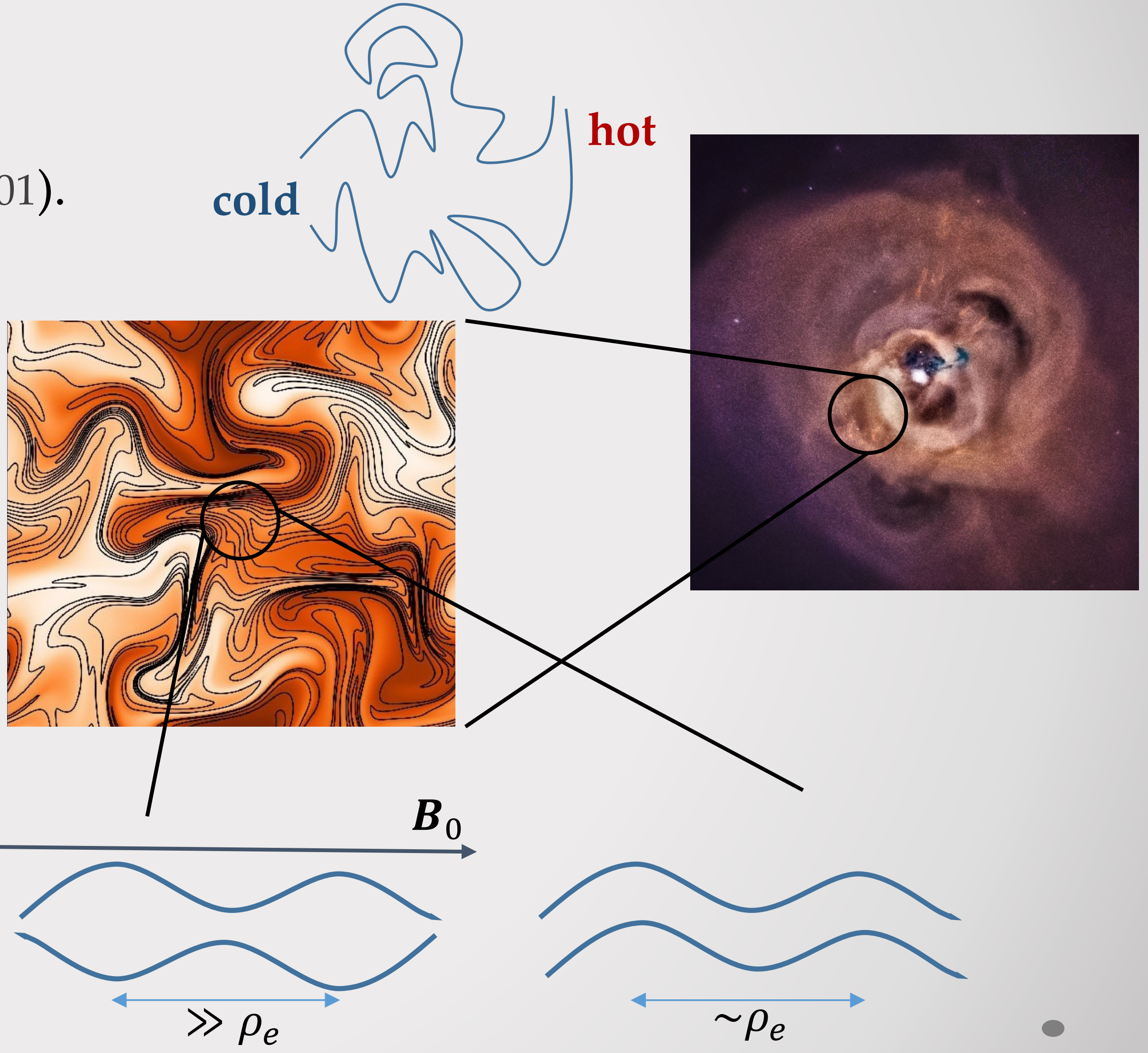

Correlation between magnetic field and temperature

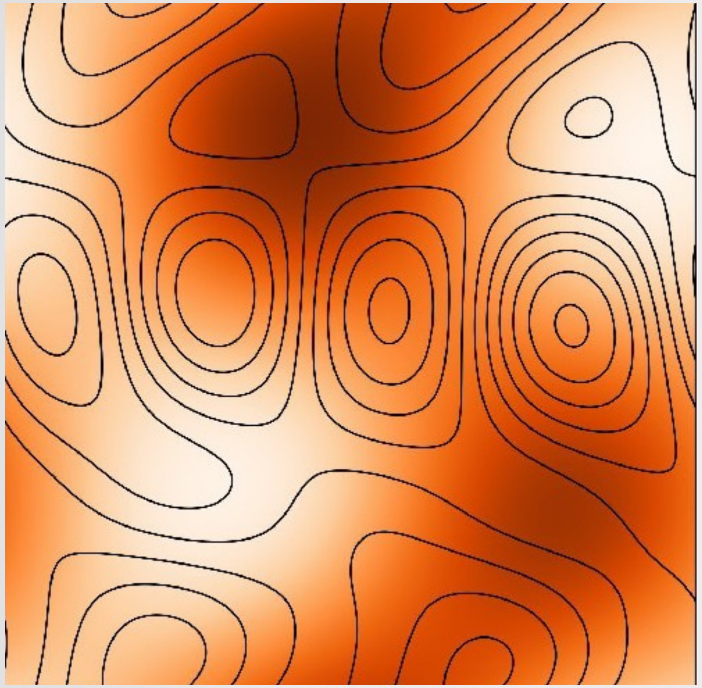

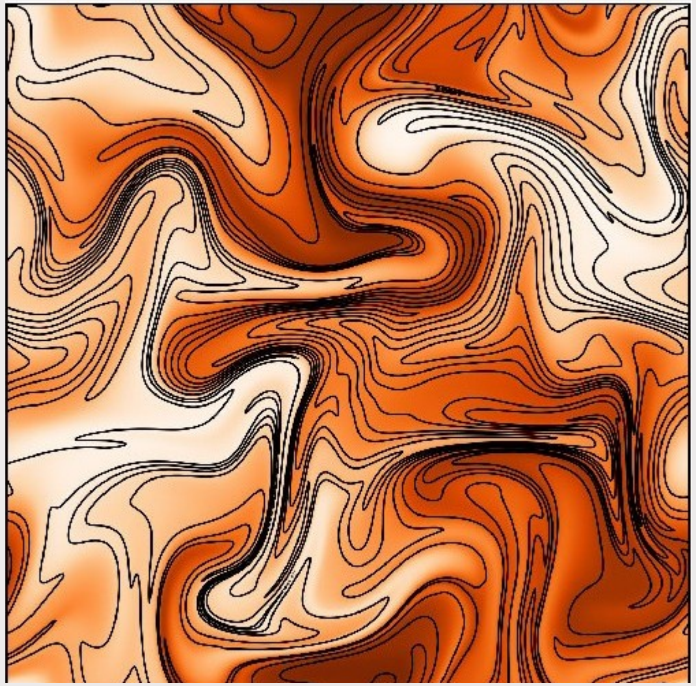

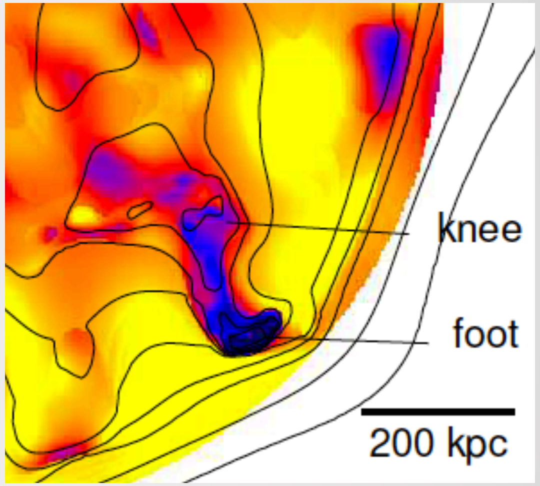

Stir 2D scalar field + 2D magnetic field (set by 2D scalar vector potential).

Magnetic isolation of regions at different temperatures or $\nabla T \perp B$.

Does it happen for "realistic" turbulent motions?

Turbulent dynamo + conduction

Pr= ν/η=Rm/Re

Pr~200, Re~3

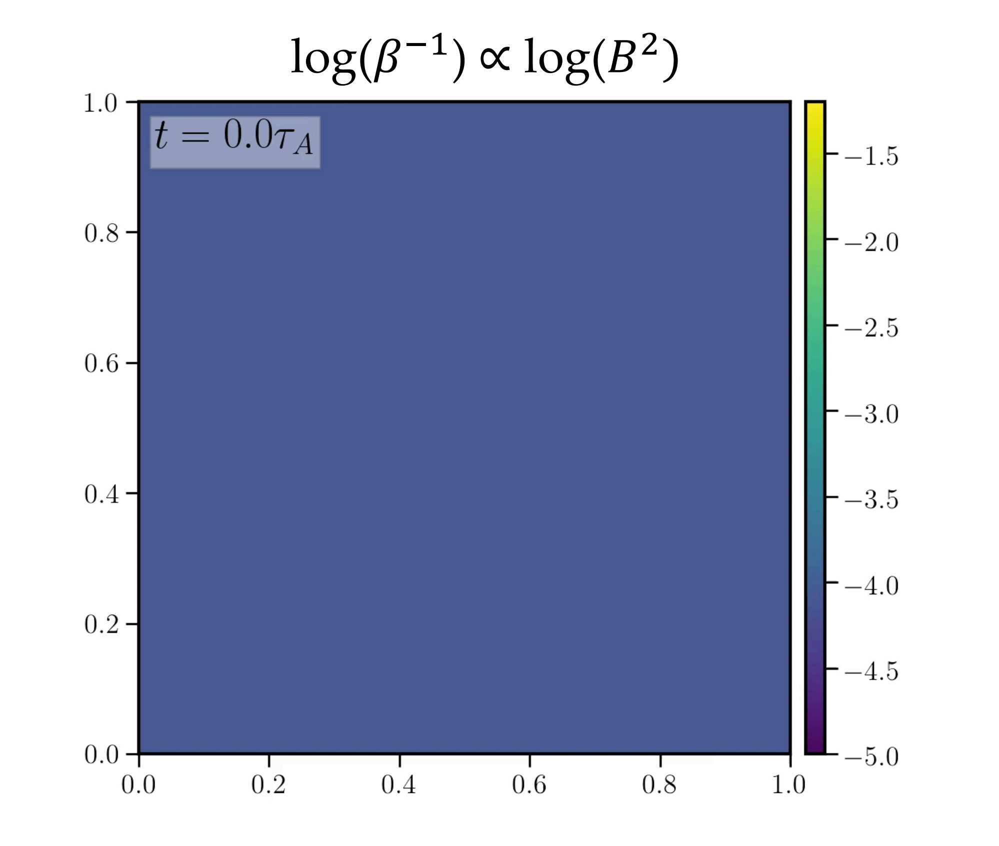

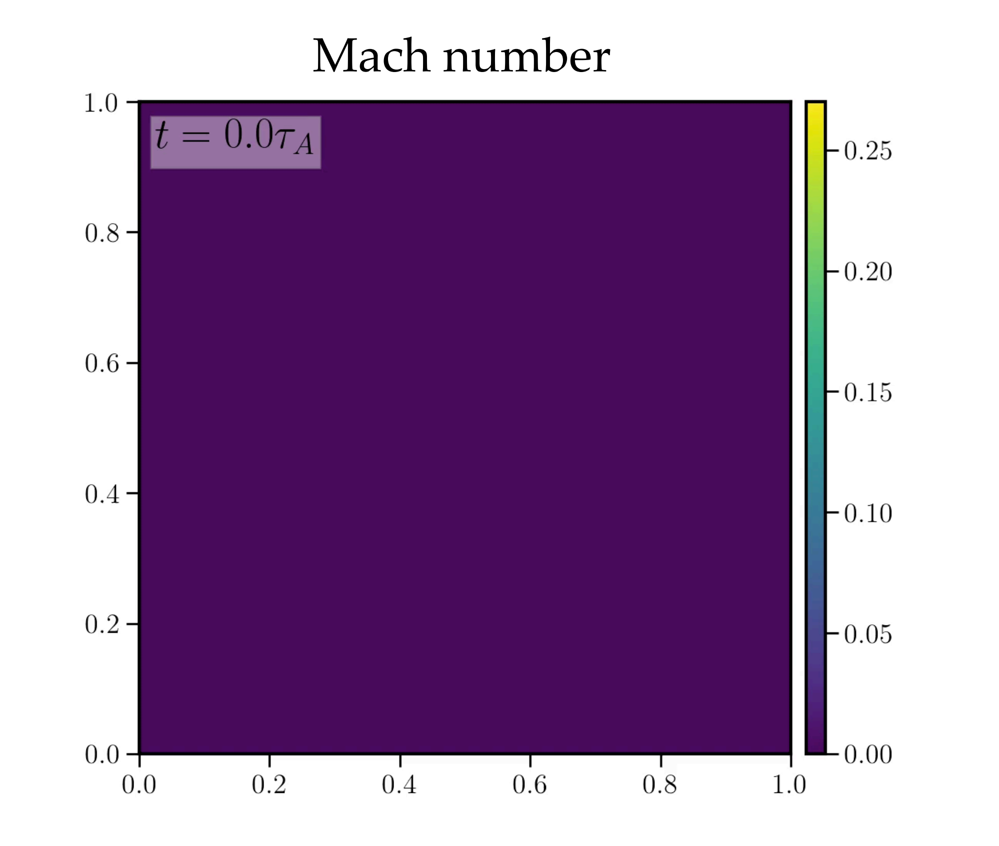

Turbulent dynamo + conduction

Pr= ν/η=Rm/Re

Pr~1, Re~400

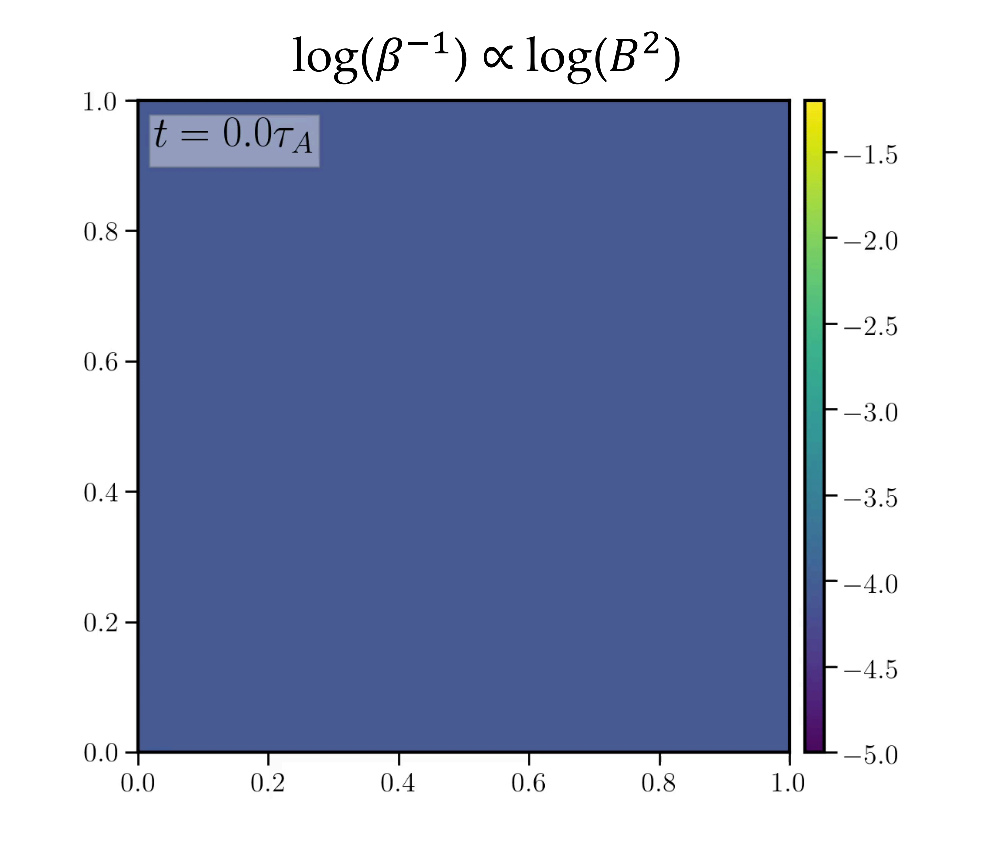

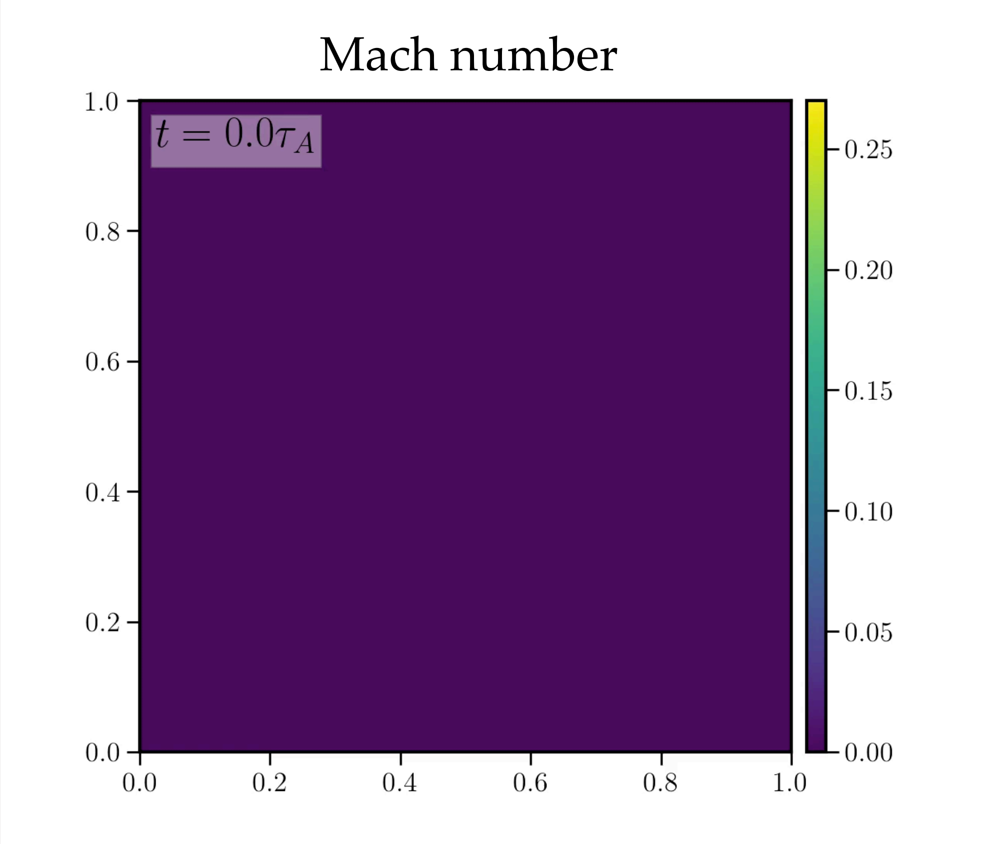

Turbulent dynamo + conduction

Introduce temperature fluctuations when dynamo is saturated:

Pr~100, Re~5

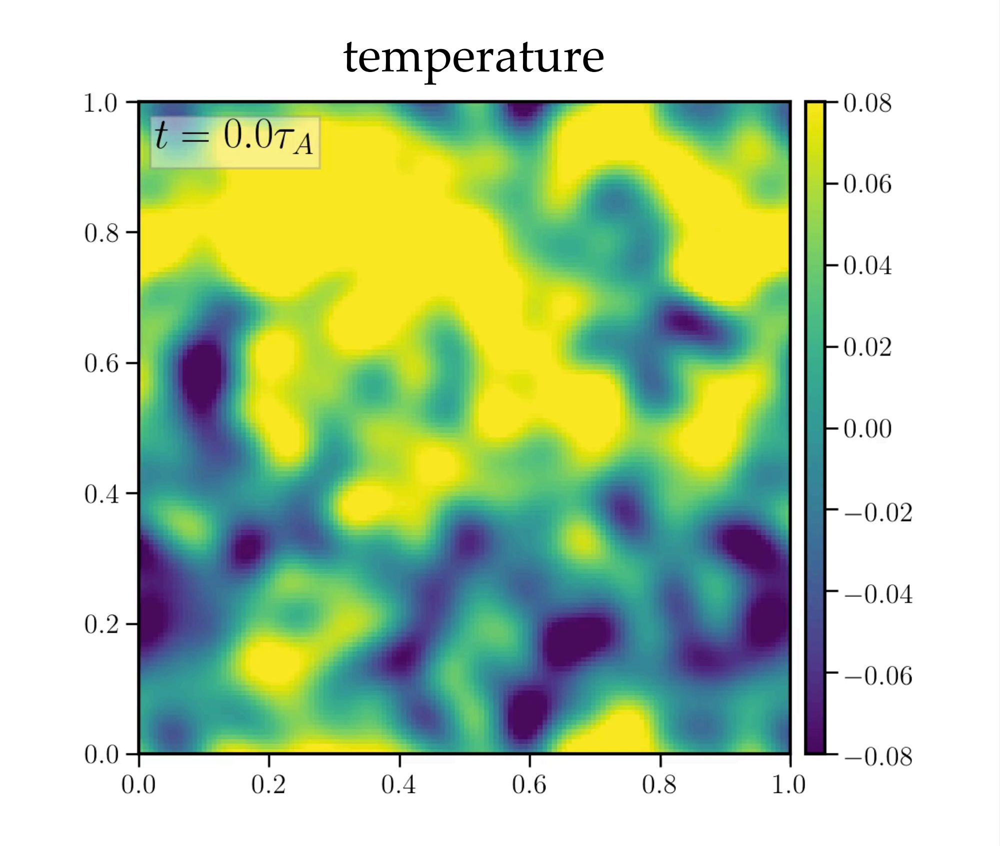

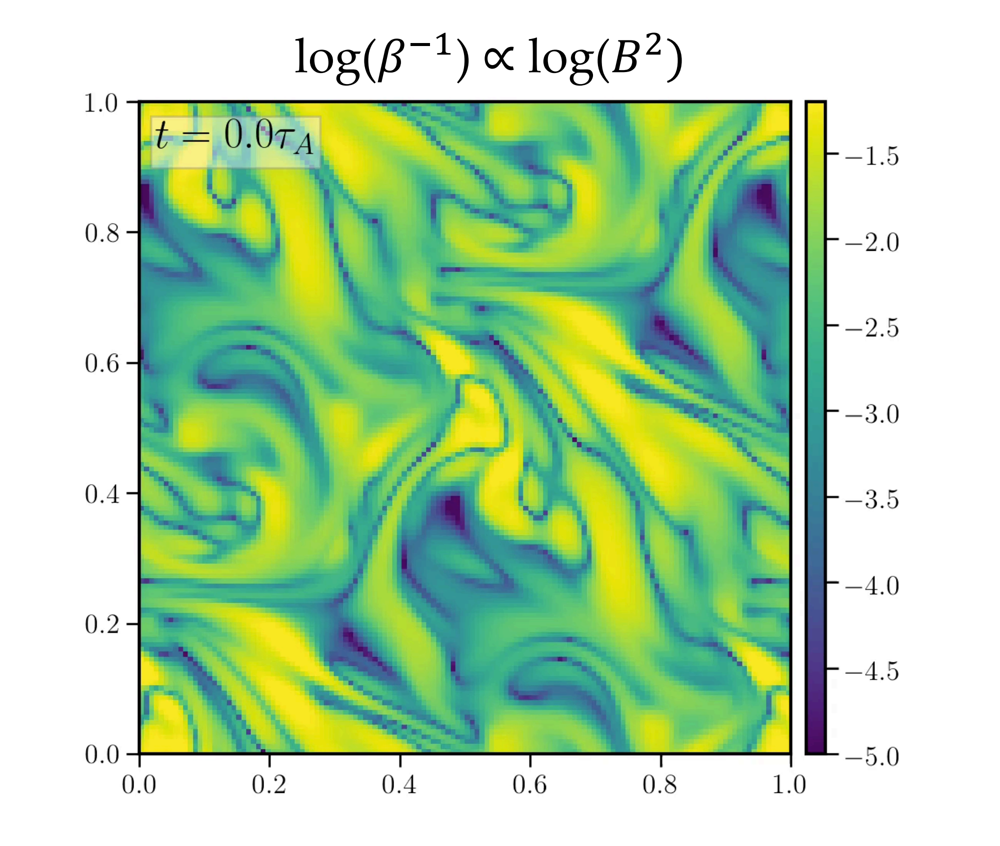

set $t_{cond} \sim L_u/u$

Turbulent dynamo + conduction

Introduce temperature fluctuations when dynamo is saturated:

Pr~1, Re~400

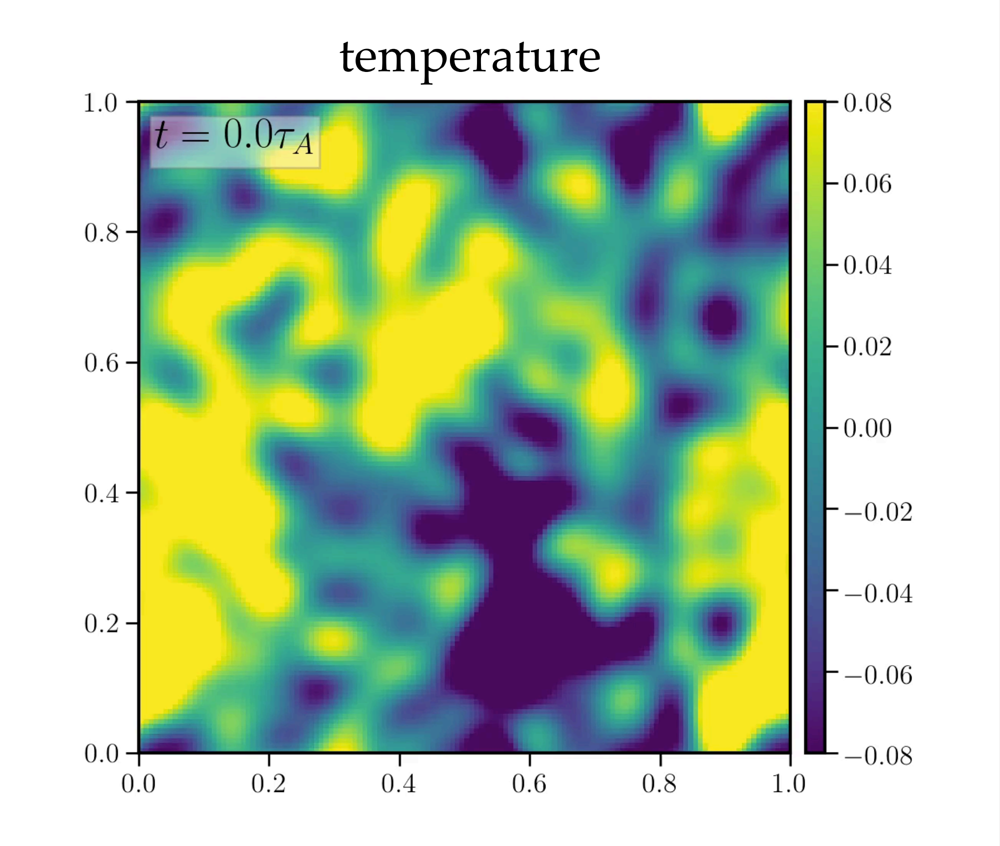

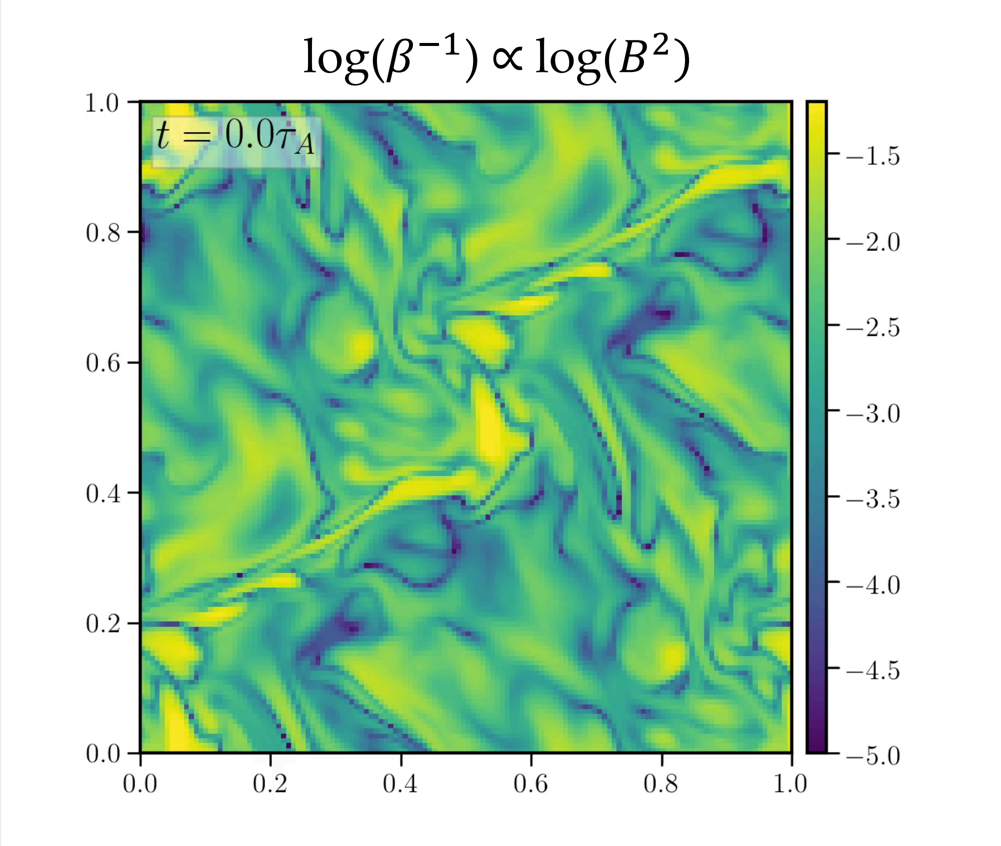

set t_{cond}~L_u/u

Turbulent dynamo + conduction

- High-Pr turbulence inhibits relaxation of temperature fluctuations by aligning $\nabla T \perp B$.
- At low Pr turbulent diffusion enhances heat exchange

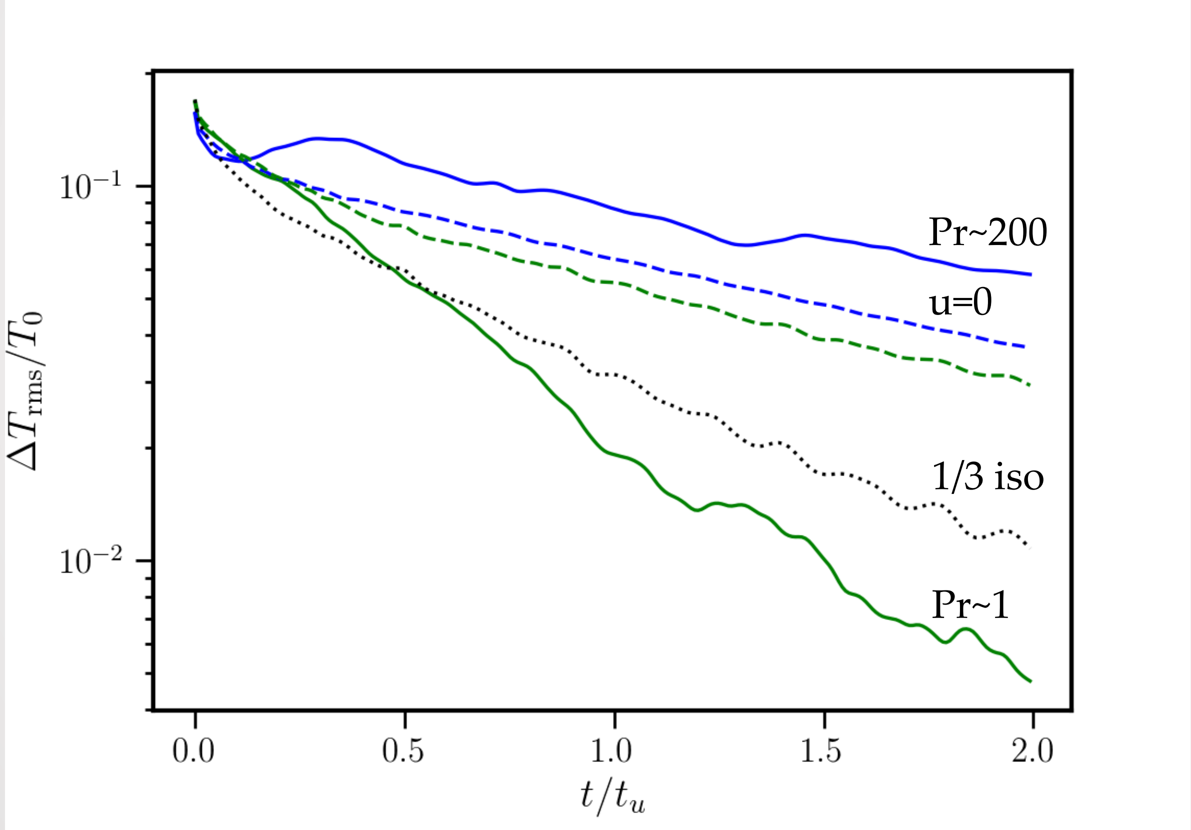

Turbulent dynamo + conduction

- High-Pr turbulence inhibits relaxation of temperature fluctuations by aligning $\nabla T \perp B$.
- At low Pr turbulent diffusion enhances heat exchange

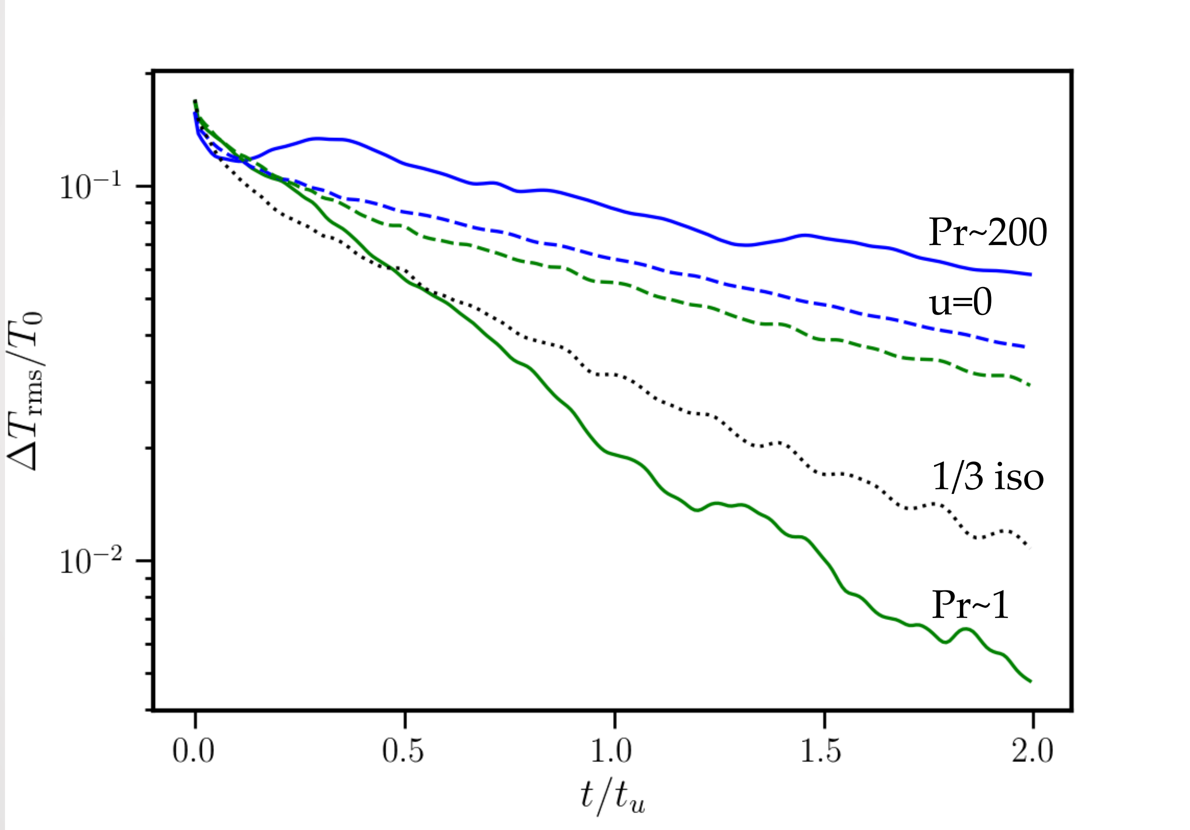

simulation of collisionless dynamo
St-Onge+ 2018

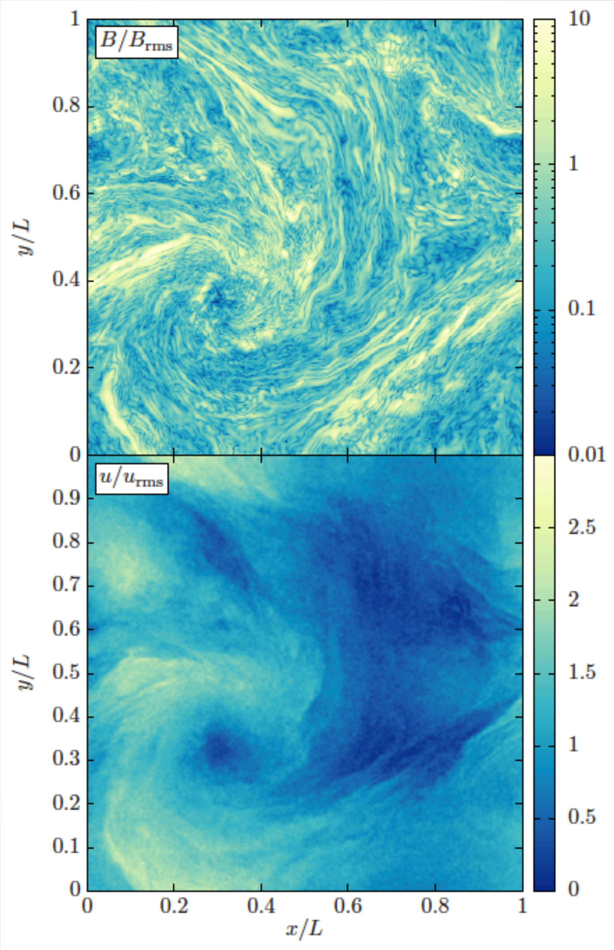

Outline

- Efficiency of thermal conduction in the ICM
- Suppression mechanisms
  - Local suppression by turbulence
  - Mirror instability
  - Whistler instability
- Summary

Weak collisionality and generation of pressure anisotropy

$$\nu_{ii} \ll \Omega_{ci} = \frac{eB}{mc}$$

$$\Downarrow$$

conservation of adiabatic invariants

$$\mu = u_\perp^2 / B = \mathrm{const}$$

$$\Downarrow$$

$p_\perp \neq p_\parallel$ pressure anisotropy

$$\frac{1}{p_\perp}\frac{\mathrm{d}p_\perp}{\mathrm{d}t} = \frac{1}{B}\frac{\mathrm{d}B}{\mathrm{d}t} - \nu\frac{p_\perp - p_\parallel}{p_\perp}$$

$$\Delta \equiv \frac{p_\perp - p_\parallel}{p_\perp} \sim \frac{1}{\nu}\frac{1}{B}\frac{\mathrm{d}B}{\mathrm{d}t} = \frac{\gamma}{\nu}$$

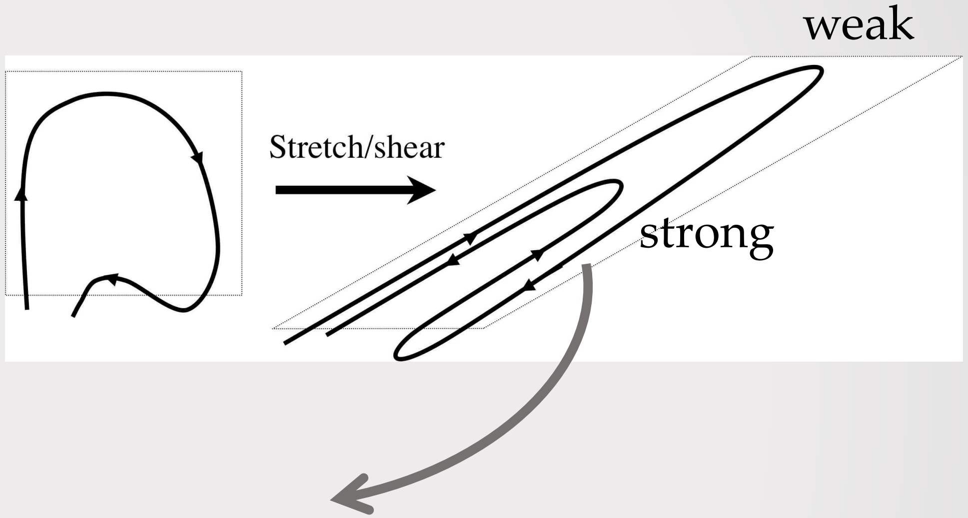

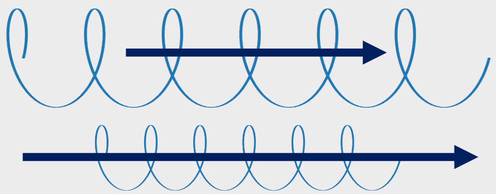

$$\frac{\mathrm{dB}}{\mathrm{dt}} = (\hat{\mathbf{b}}\hat{\mathbf{b}} : \nabla\mathbf{u})B \equiv \gamma B$$

Mirror instability

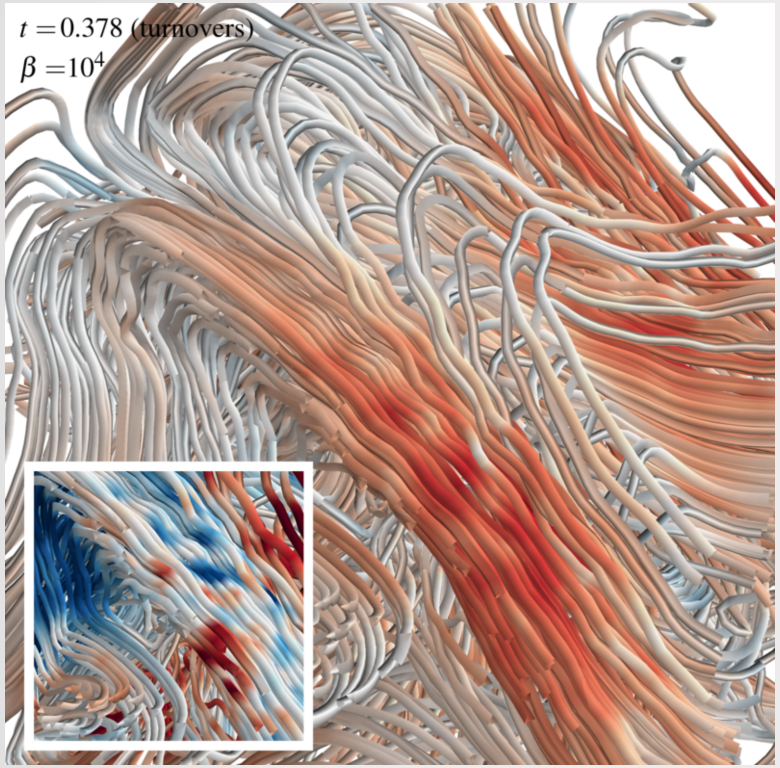

kinetic simulation of turbulent dynamo

Rincon et al. 2016

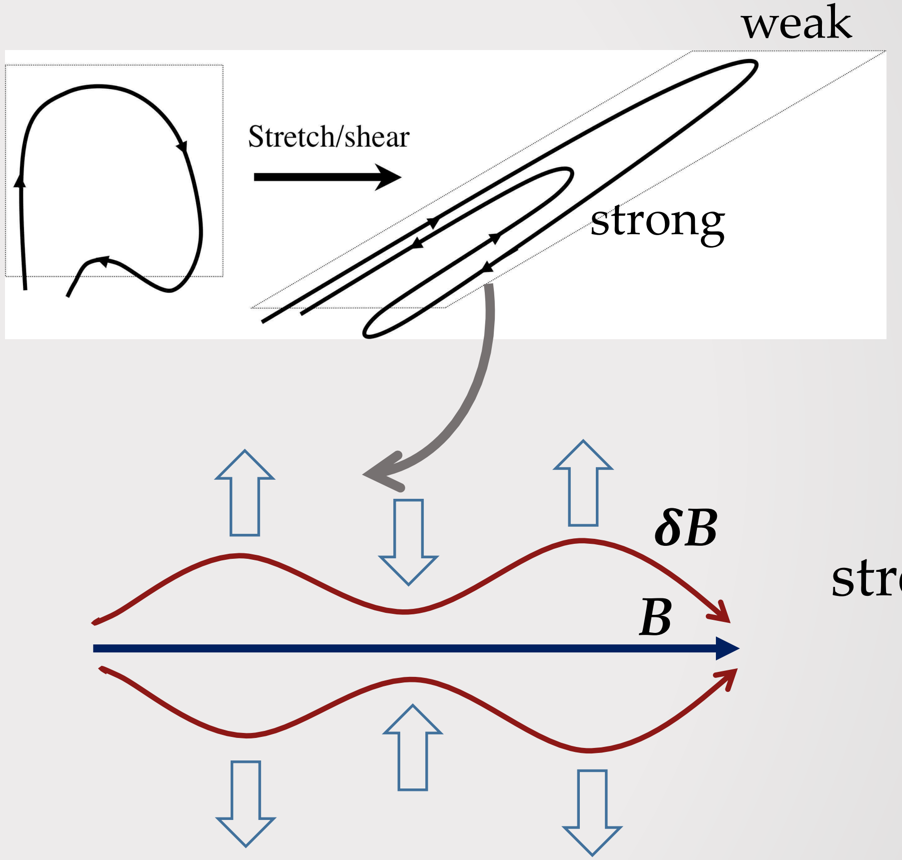

stretching $\boldsymbol{B}$

$p_\perp > p_\parallel$

$$\delta p_\perp = -2p_\perp \underbrace{(p_\perp/p_\parallel - 1)}_{\substack{\parallel \\ \Delta > 1/\beta}} \delta B/B$$

$\Delta > 1/\beta$ instability

Mirror instability

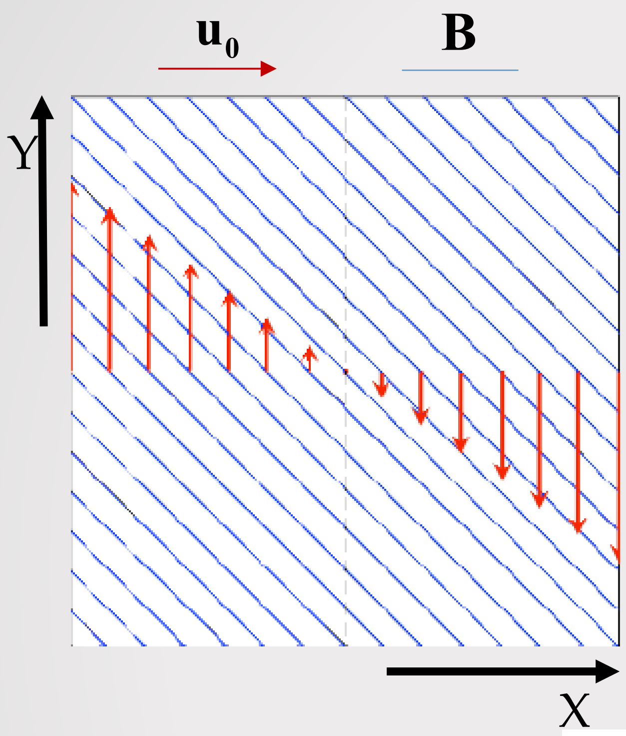

$$\frac{dB}{dt} > 0$$

$$\Delta = \frac{p_\perp - p_\parallel}{p_\perp} > 0$$

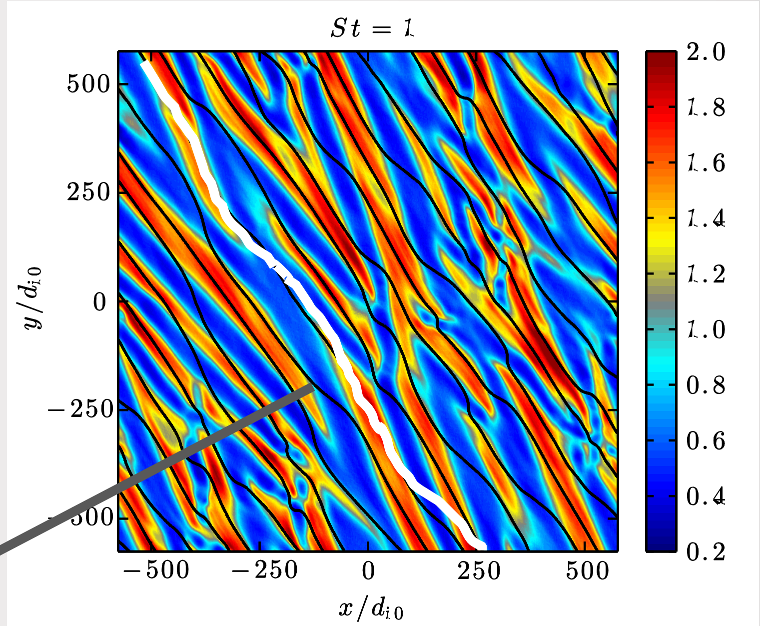

Kunz et al. 2014

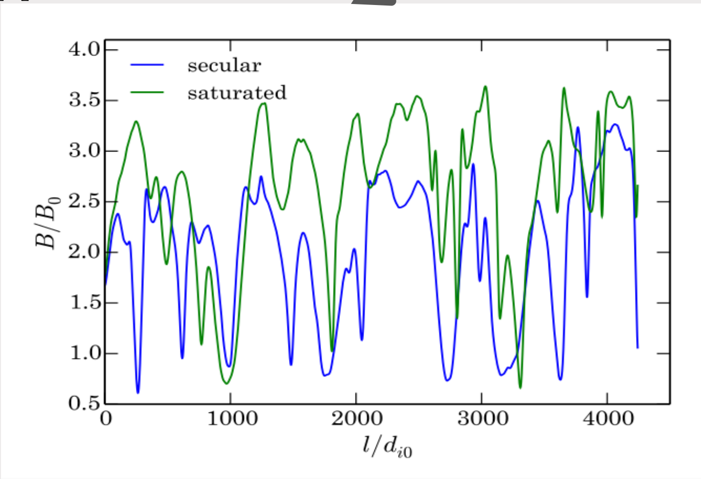

field strength
along a field line

Mirror instability

Diffusion in magnetic mirrors in presence of weak collisions

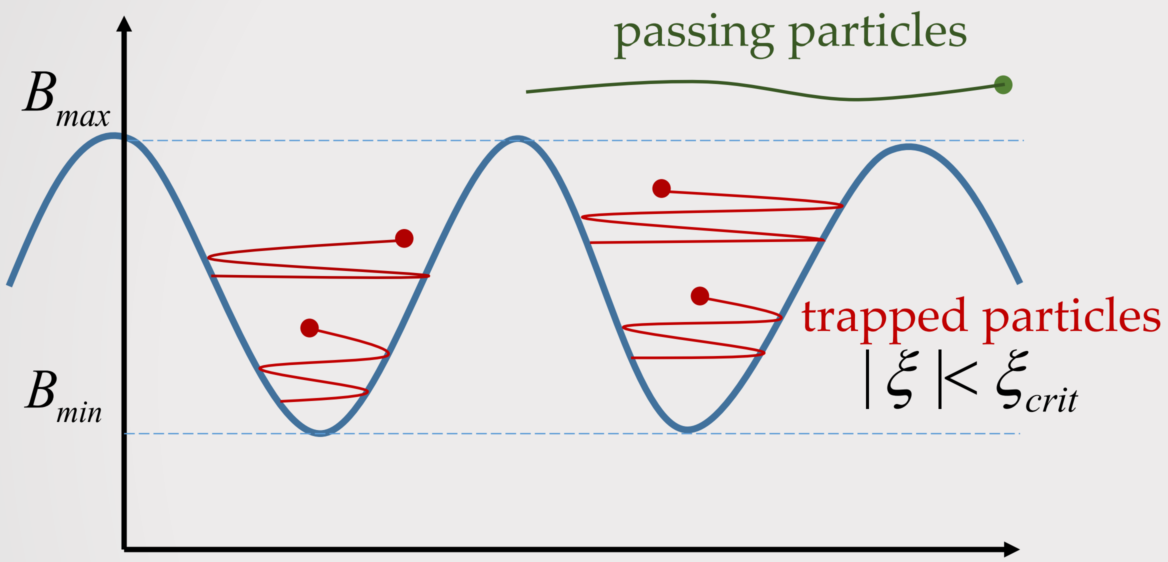

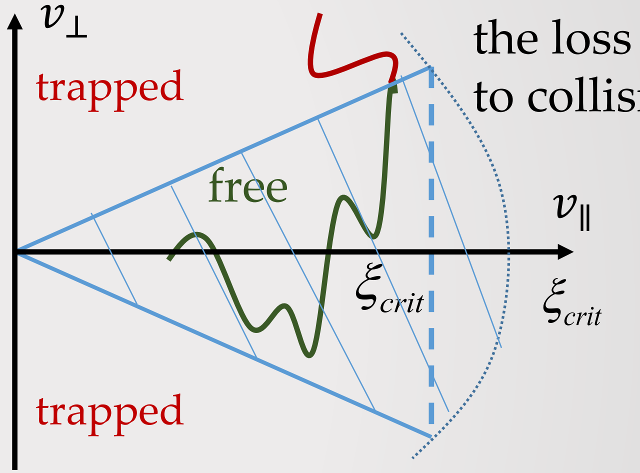

Mirror instability

Diffusion in magnetic mirrors in presence of weak collisions

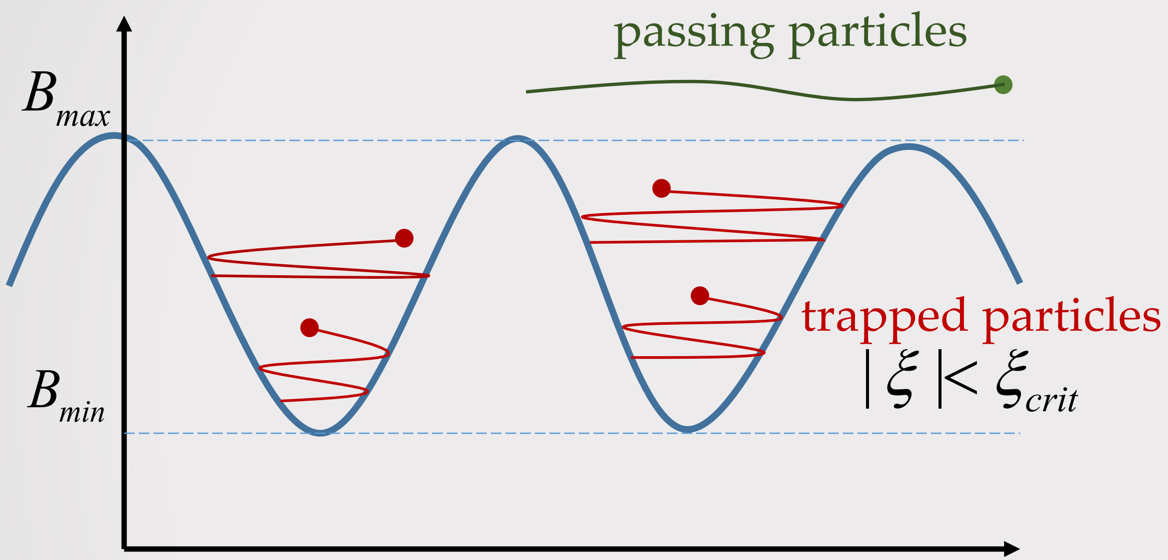

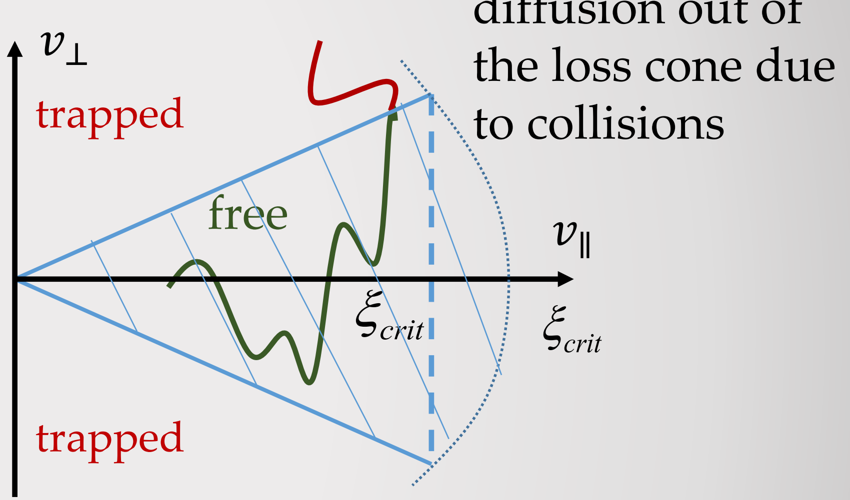

Monte Carlo modeling of 1D particle motion in static mirrors in presence of weak collisions

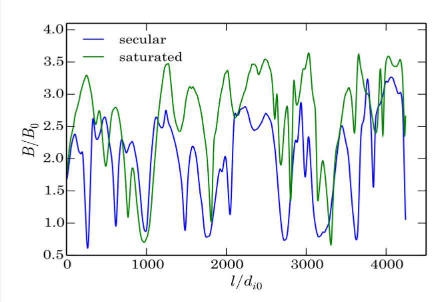

1/10 suppression of electron diffusion

1/5 suppression of electron conduction

Outline

- Efficiency of thermal conduction in the ICM

- Suppression mechanisms
  - Local suppression/enhancement by turbulence
  - Mirror instability
  - Whistler instability

- Summary

Heat-flux-induced whistler instability

heat flux <-> asymmetry of electron distribution function

$f = f_0 + \varepsilon f_1, \varepsilon = \lambda_{mfp}/L_T \quad q_\parallel \sim n_e \lambda_{mfp} v_{th} T/L_T \sim \varepsilon m_e n_e v_{th}^3$

Maxwell → f_0 perturbation → f_1

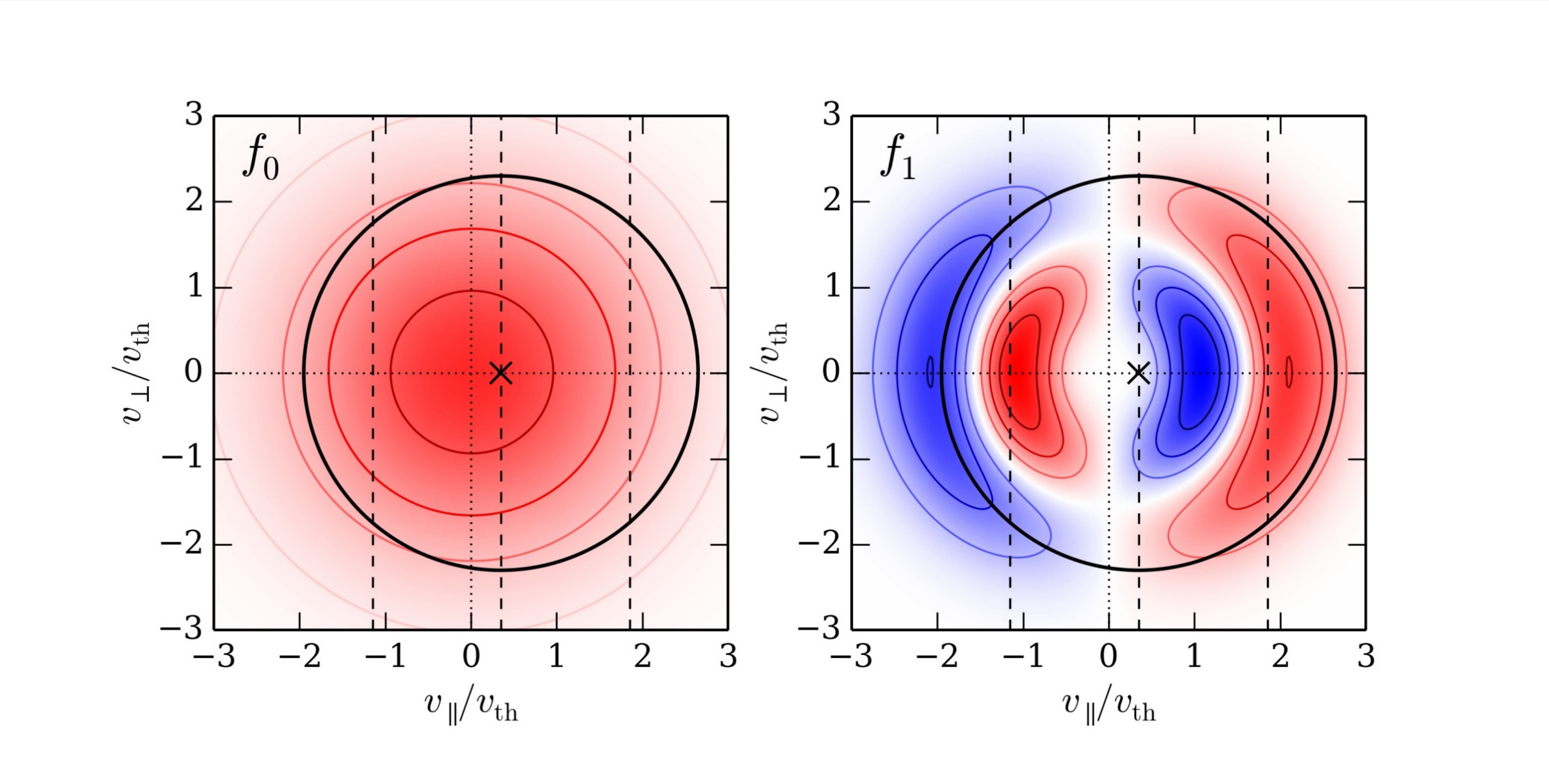

Heat-flux-induced whistler instability

heat flux <-> asymmetry of electron distribution function

$$f = f_0 + \varepsilon f_1, \varepsilon = \lambda_{mfp}/L_T \quad q_{\parallel} \sim \varepsilon m_e n_e v_{th}^3$$

Maxwell

perturbation

wave phase speed

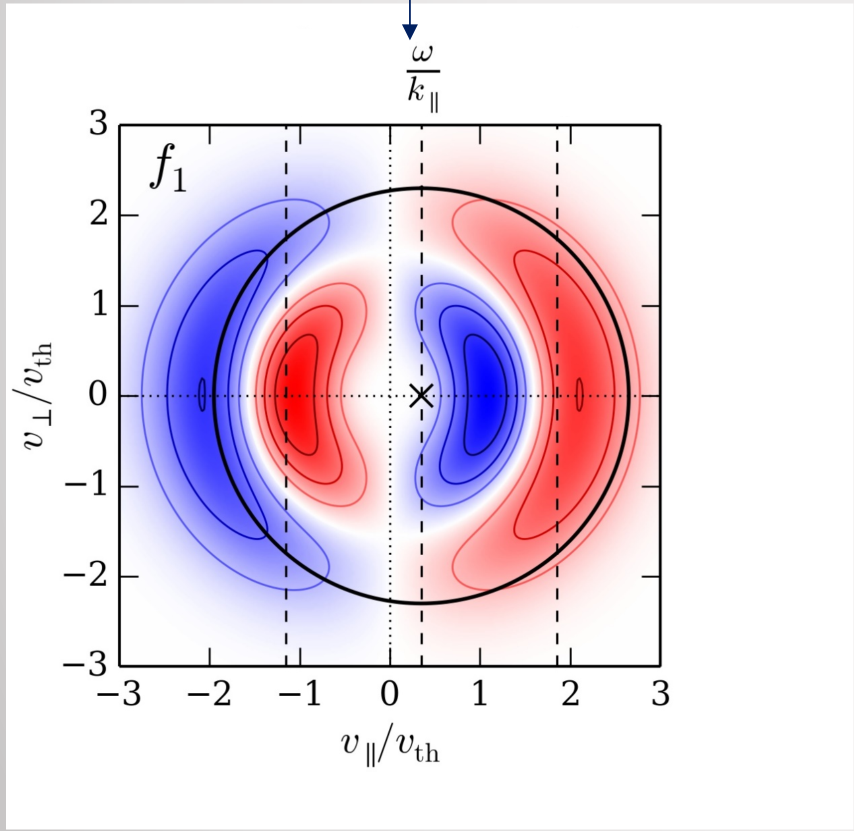

transverse whistler wave along field

$\omega/k \ll v_{th,e}$

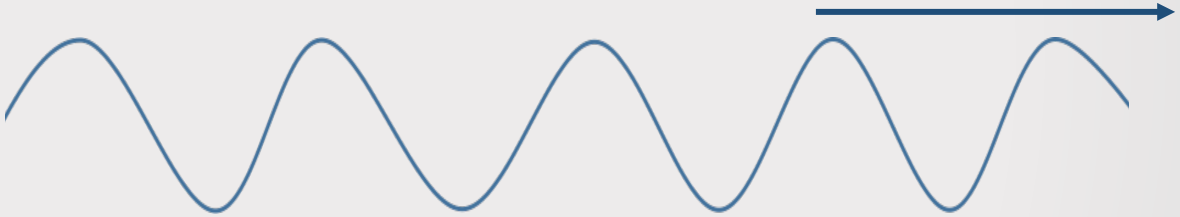

Heat-flux-induced whistler instability

heat flux <-> asymmetry of electron distribution function

$$f = f_0 + \varepsilon f_1, \varepsilon = \lambda_{mfp}/L_T \quad q_\parallel \sim \varepsilon m_e n_e v_{th}^3$$

Maxwell

perturbation

wave phase speed

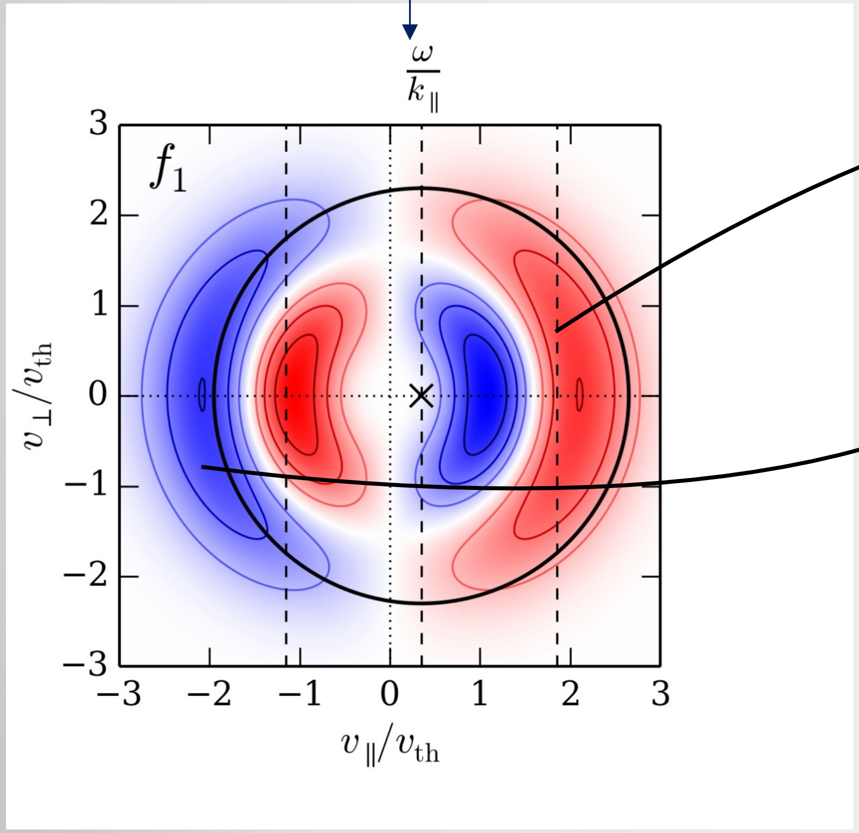

heat-carrying e⁻
have excess of $p_\parallel$

transverse whistler
wave along field
$\omega/k \ll v_{th,e}$

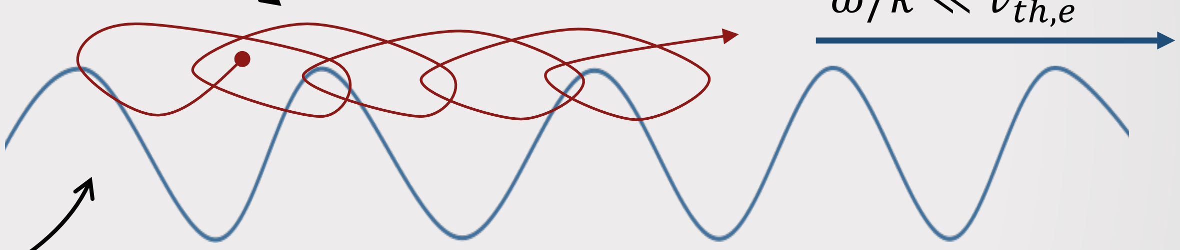

take resonant wave that scatters particles ->

Heat-flux-induced whistler instability

heat flux <-> asymmetry of electron distribution function

$$f = f_0 + \varepsilon f_1, \varepsilon = \lambda_{mfp}/L_T \qquad q_\parallel \sim \varepsilon m_e n_e v_{th}^3$$

Maxwell

perturbation

gyroresonances

wave phase speed

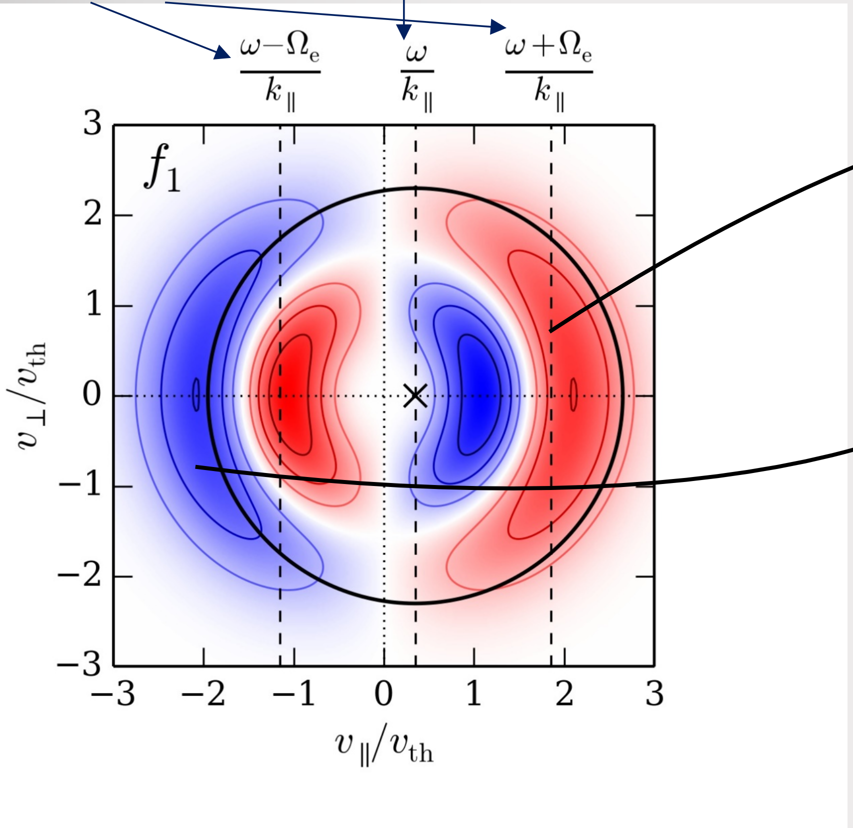

heat-carrying e$^-$ have excess of $p_\parallel$

transverse whistler wave along field

$\omega/k \ll v_{th,e}$

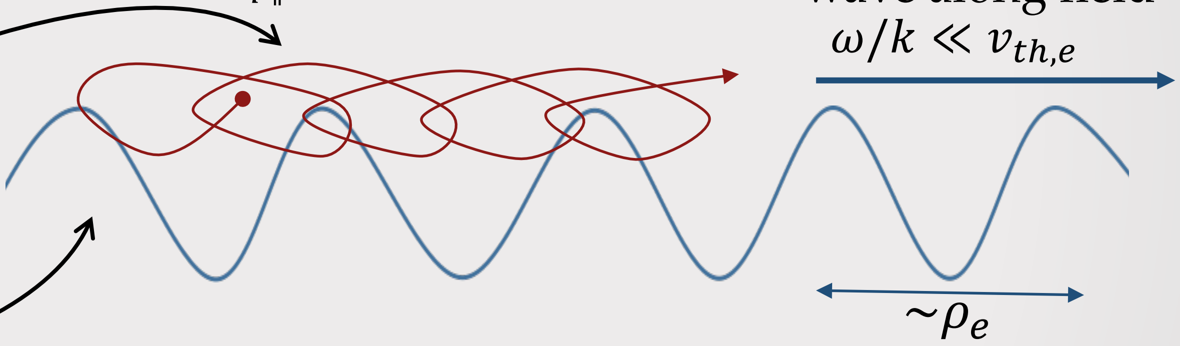

resonant scattering condition:

$$\omega - k_\parallel v_\parallel = \pm\Omega_e$$

$$k_\parallel \sim \rho_e^{-1}$$

Heat-flux-induced whistler instability

heat flux <-> asymmetry of electron distribution function

$$f = f_0 + \varepsilon f_1, \varepsilon = \lambda_{mfp}/L_T \quad q_\parallel \sim \varepsilon m_e n_e v_{th}^3$$

Maxwell perturbation

wave phase speed

gyroresonances

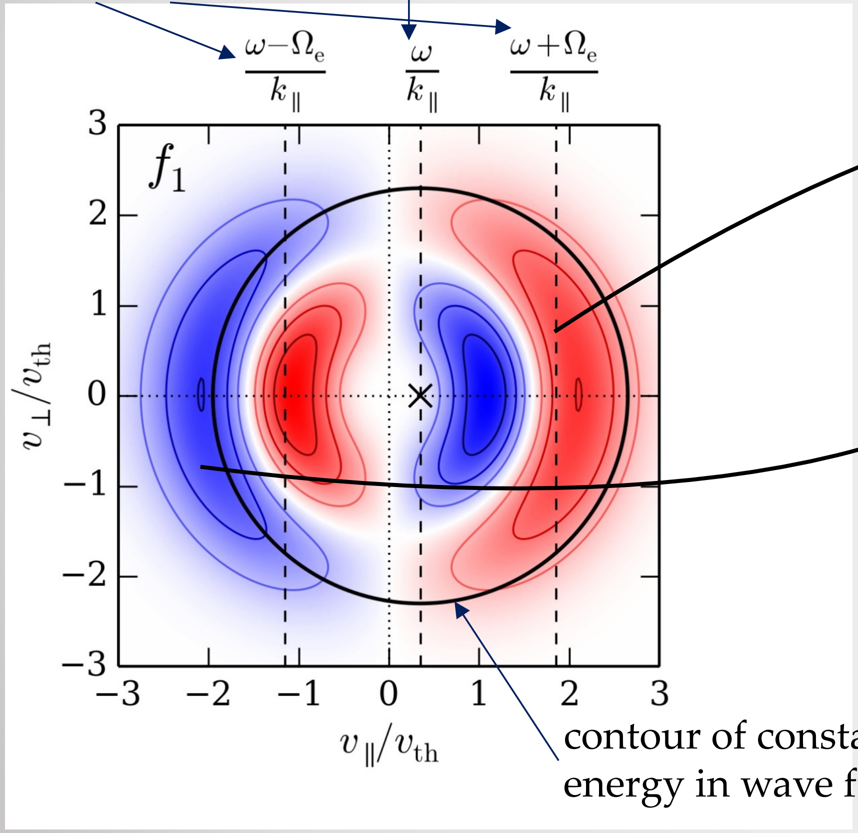

contour of constant energy in wave frame

heat-carrying e⁻ have excess of $p_\parallel$

transverse whistler wave along field $\omega/k \ll v_{th,e}$

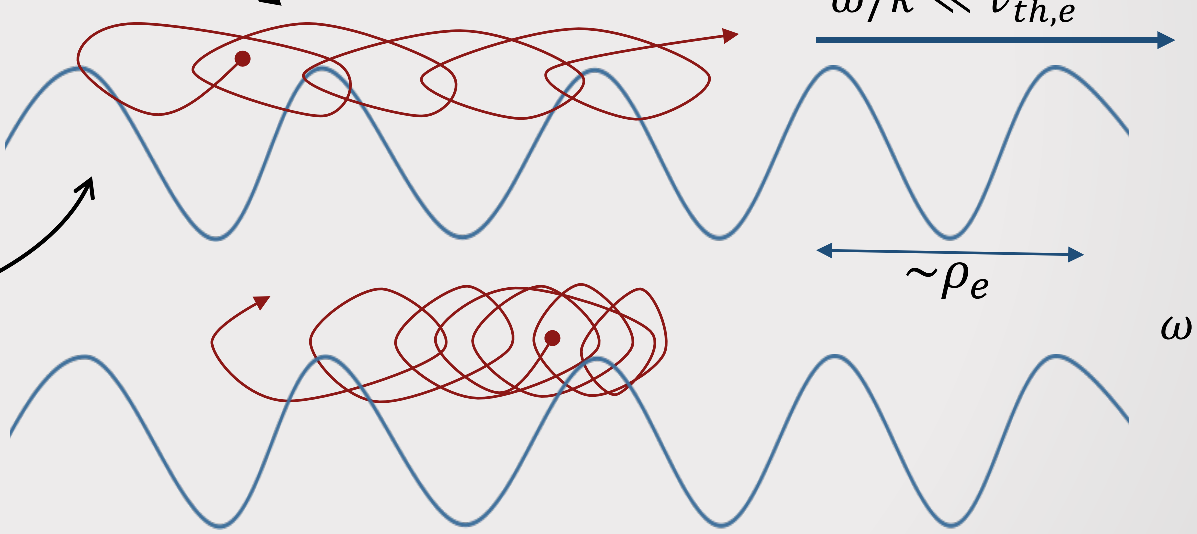

resonant scattering condition:

$$\omega - k_\parallel v_\parallel = \Omega_e$$

$$k_\parallel \sim \rho_e^{-1}$$

energy is conserved in wave frame –> loss of initial parallel momentum, energy transferred to wave

Marginal heat flux

heat flux <-> asymmetry of electron distribution function

$$f = f_0 + \varepsilon f_1, \varepsilon = \lambda_{mfp}/L_T \quad q_{\|} \sim \varepsilon m_e n_e v_{th}^3$$

Maxwell $\rightarrow f_0$ perturbation $\rightarrow f_1$

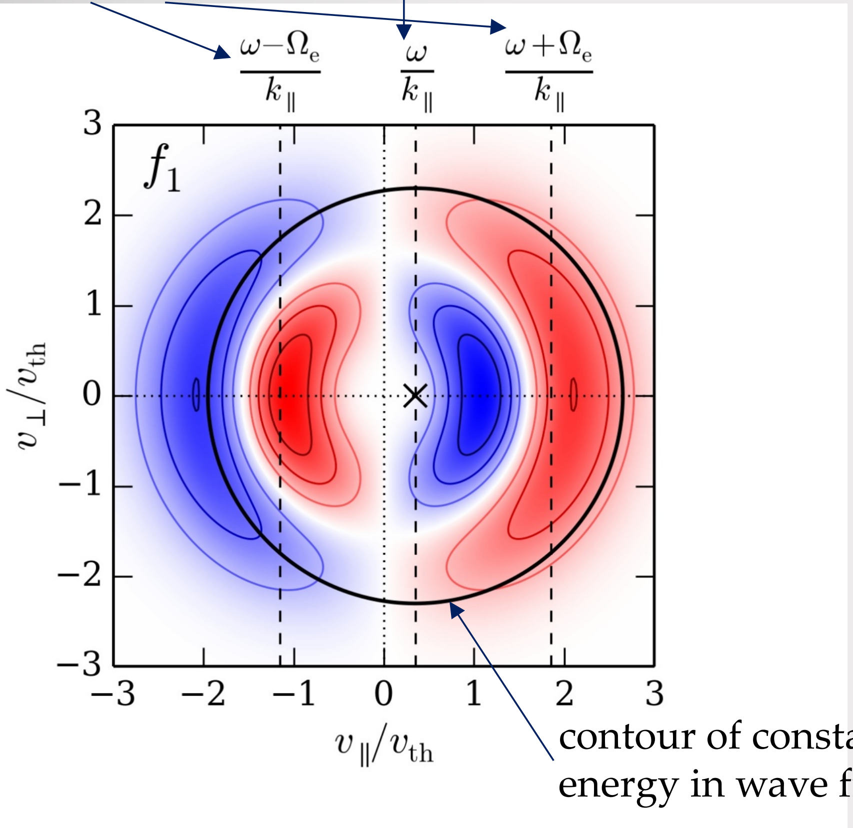

from dispersion relation at $k_\| \sim \rho_e^{-1}$:

$$\omega/k_\| \sim v_{th,e}/\beta \ll v_{th,e}$$

in galaxy clusters $\beta \sim 100$

over time, electrons become isotropic in wave frame -> energy exchange stops:

$$\left[(v_\| - \omega/k_\|)\frac{\partial}{\partial v_\perp} - v_\perp \frac{\partial}{\partial v_\|}\right] \mathrm{f}(\mathbf{v}) = 0$$

$$\frac{v_{th}}{\beta}\underbrace{\frac{\partial f_0}{\partial v}}_{\sim f_0/v_{th}} - \varepsilon \underbrace{\frac{\partial f_1}{\partial \xi}}_{\sim f_0} = 0 \longrightarrow \varepsilon\beta = 1$$

using heat flux ->

$$\boxed{q_\| \sim \beta^{-1} m_e n_e v_{th}^3}$$

Oblique vs. parallel

$$f = f_0 + \varepsilon f_1, \varepsilon = \lambda_{mfp}/L_T \quad q_\parallel \sim \varepsilon m_e n_e v_{th}^3$$

parallel whistlers have **E** rotating opposite to gyration of cold-ward electrons!

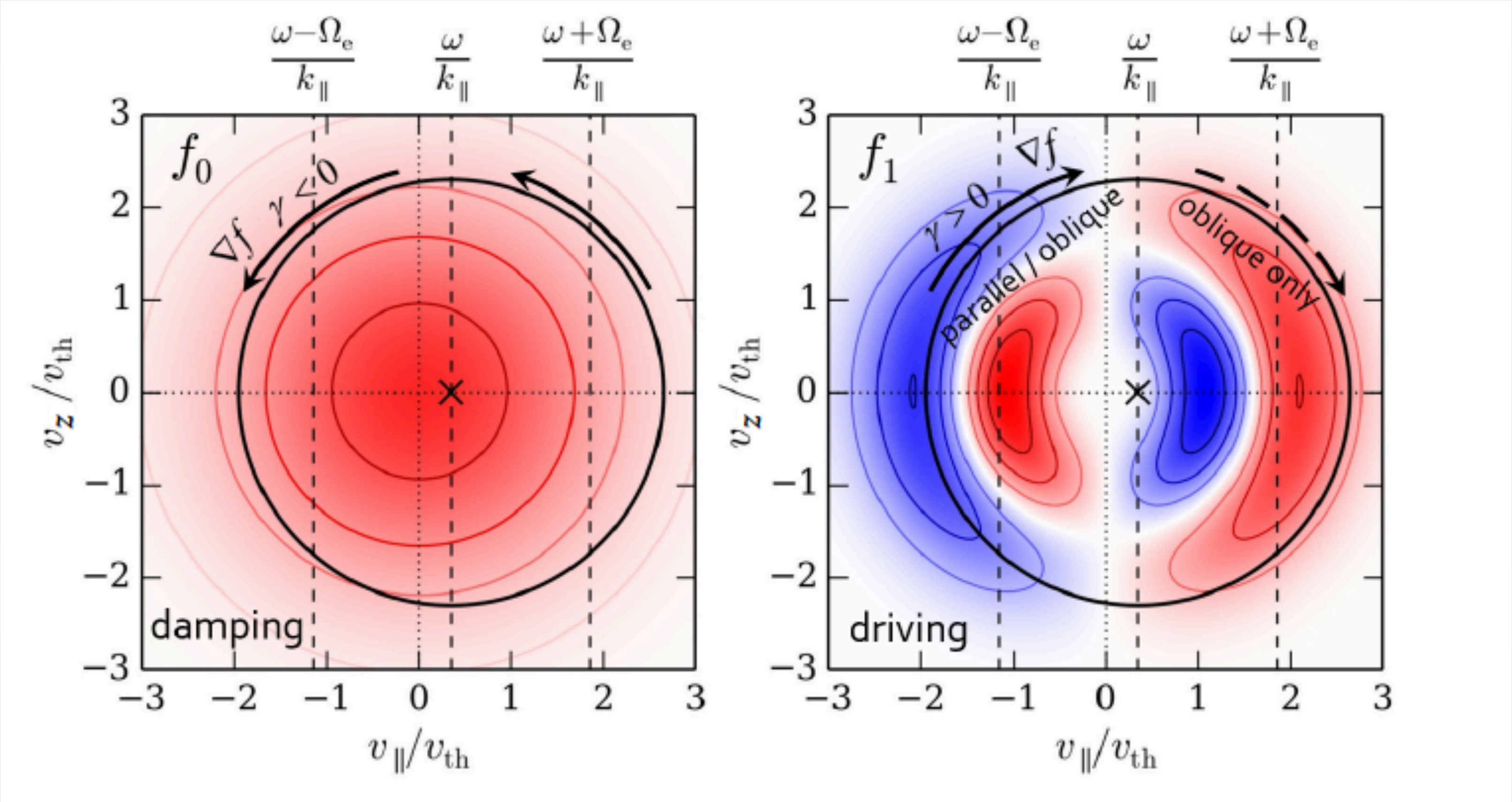

$$\varepsilon\beta = 1 \qquad \boxed{q_\parallel \sim \beta^{-1} m_e n_e v_{th}^3}$$

Quasilinear saturation

heat flux <-> asymmetry of electron distribution function

$$f = f_0 + \varepsilon f_1, \varepsilon = \lambda_{mfp}/L_T$$

Maxwell

perturbation

wave phase speed

gyroresonances

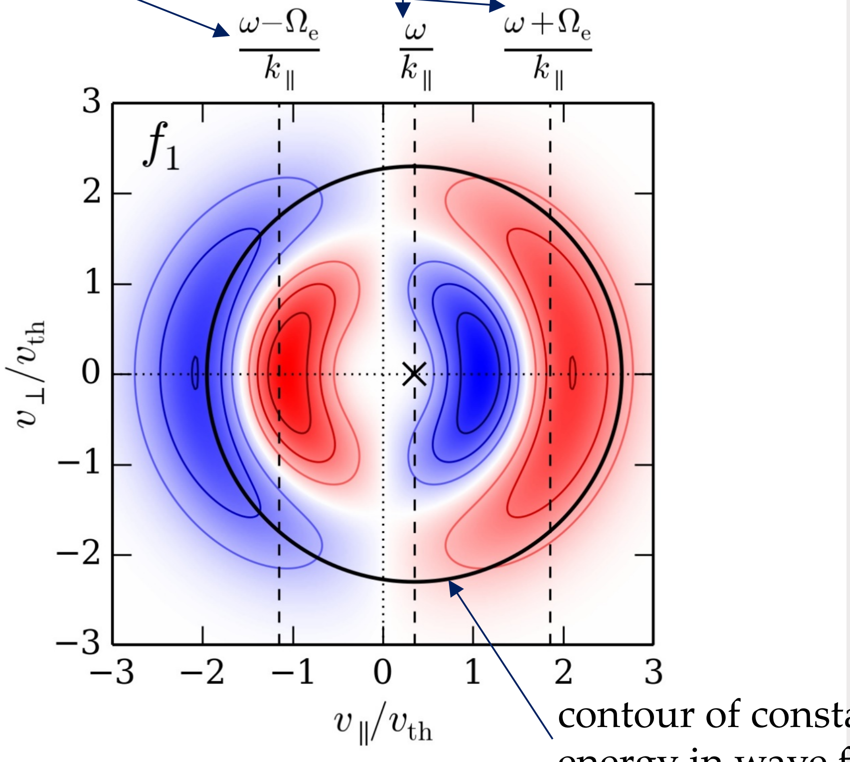

contour of constant energy in wave frame

pitch-angle diffusion:

$$\frac{\nu_{scatt}}{\Omega_e} \sim \frac{\delta B_\perp^2}{B_0^2}$$

$$\nu_{scatt} = v_{th}/\lambda_{mfp} = v_{th}/\varepsilon L_T, \ \varepsilon\beta = 1$$

$$\boxed{\frac{\delta B_\perp^2}{B_0^2} \sim \beta \frac{\rho_e}{L_T}}$$

Simulations of the instability

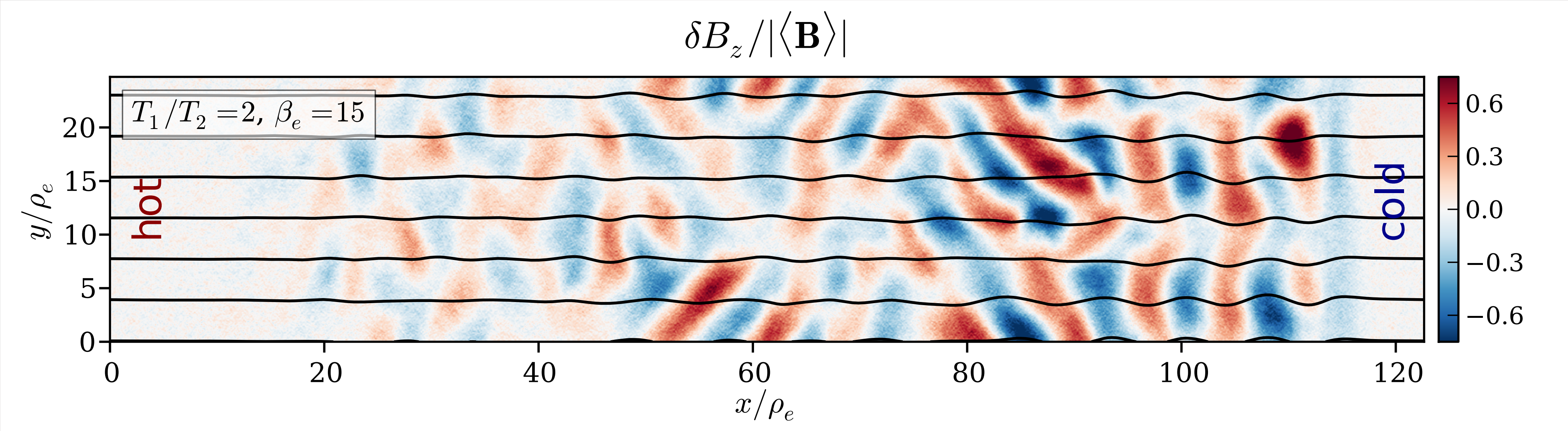

PIC code *TRISTAN* (Buneman 1993)

- Absorbing BC for waves along x
- Reflective BC for particles x:
  particle gains new velocity after reflection from wall;
  sustained temperature gradient
- Ions do not move
- Initial electron distribution is isotropic;
  particle density set to keep pressure uniform

use runs with
varying β and T_1/T_2:
$\beta = (10, 15, 25, 40)$
T_1/T_2=(1.5, 2, 3)

Simulations of the instability

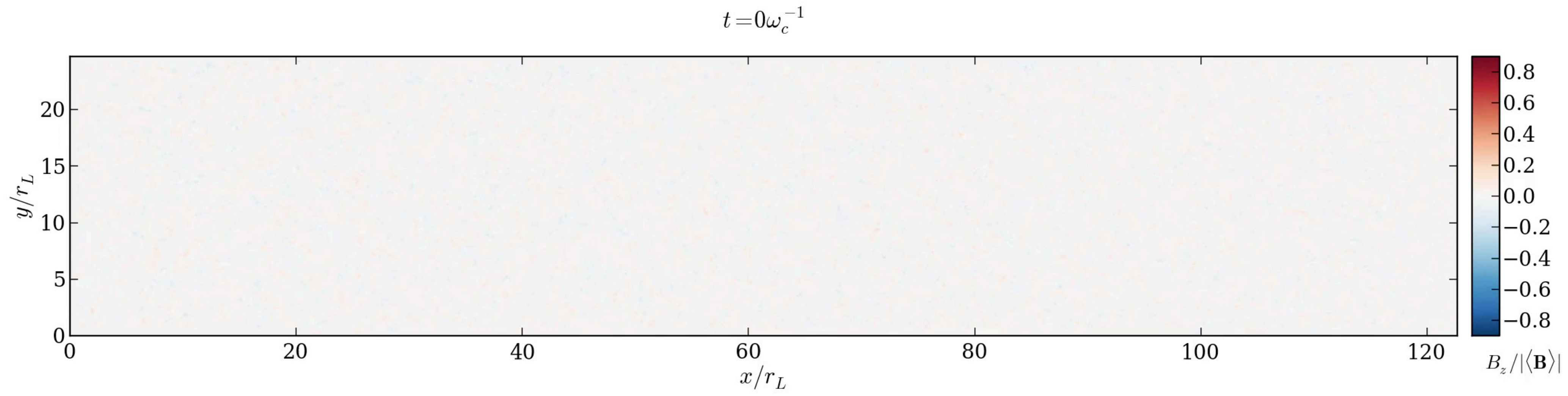

- Absorbing BC for waves along x
- Reflective BC for particles x:
  particle gains new velocity after reflection from wall;
  sustained temperature gradient
- Ions do not move
- Initial electron distribution is isotropic;
  particle density set to keep pressure uniform

use runs with
varying β and T_1/T_2:
$\beta = (10, 15, 25, 40)$
T_1/T_2=(1.5, 2, 3)

Simulations of the instability

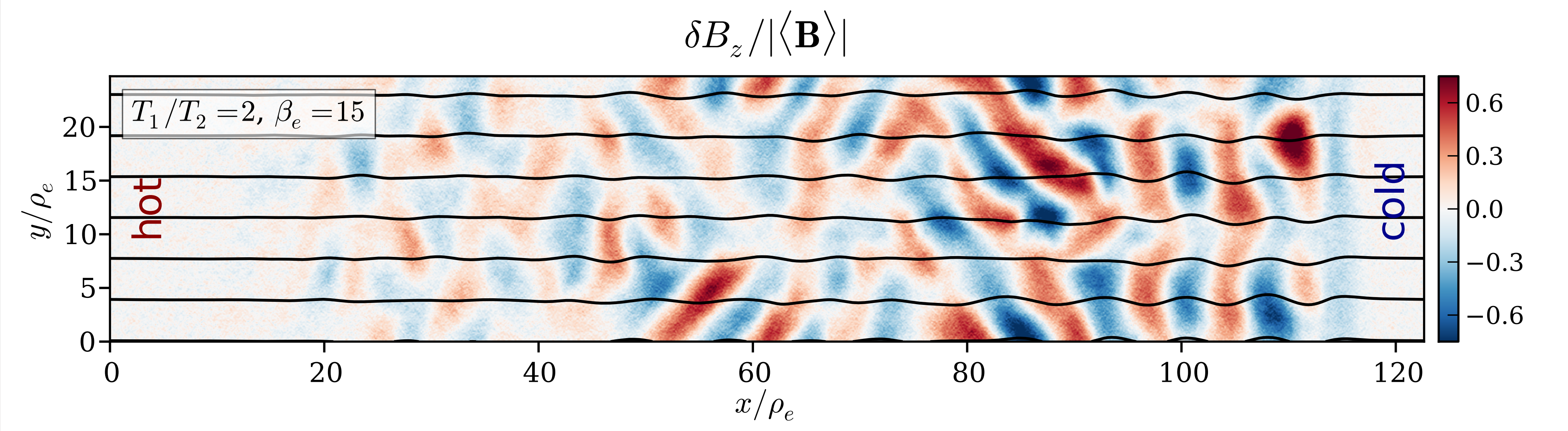

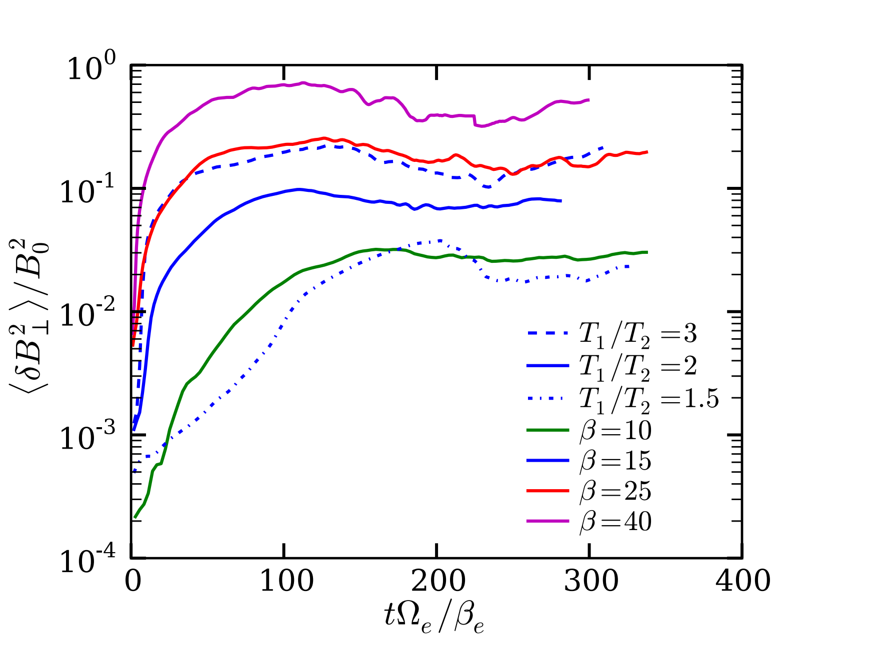

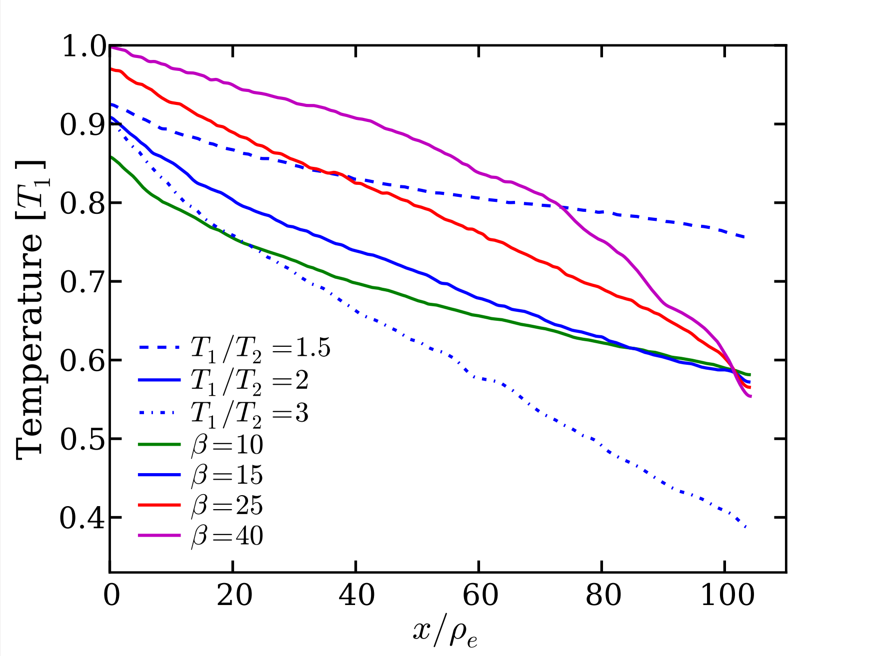

Comparison with theory

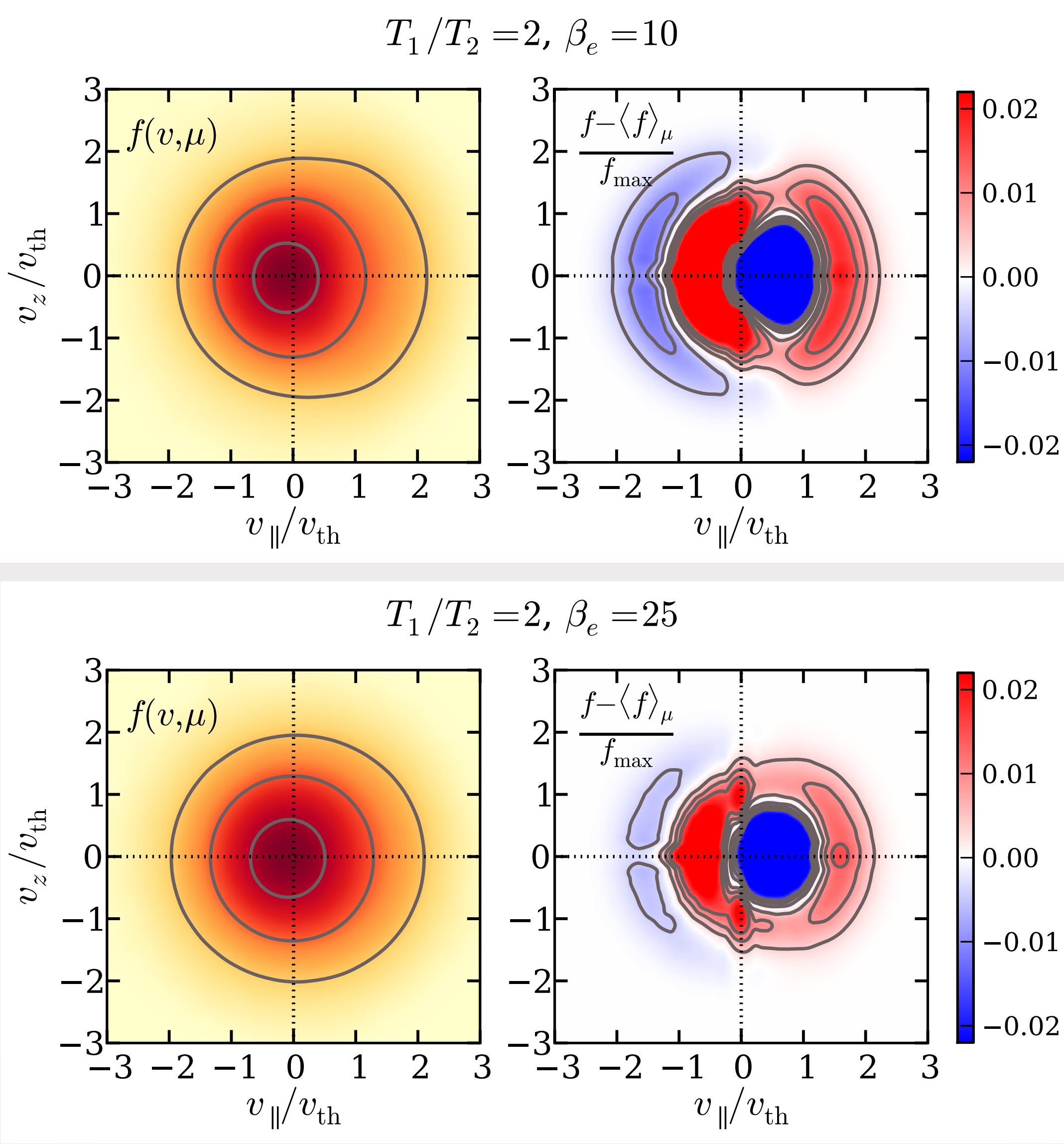

Comparison with theory

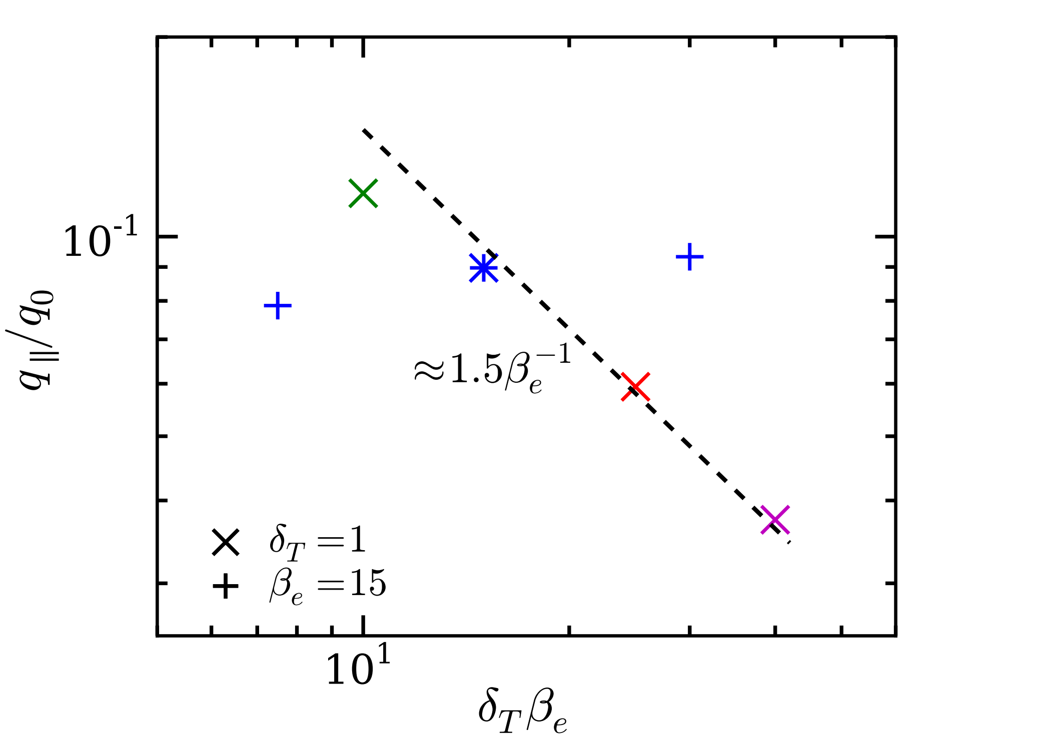

$\delta_T = T_1/T_2$-1

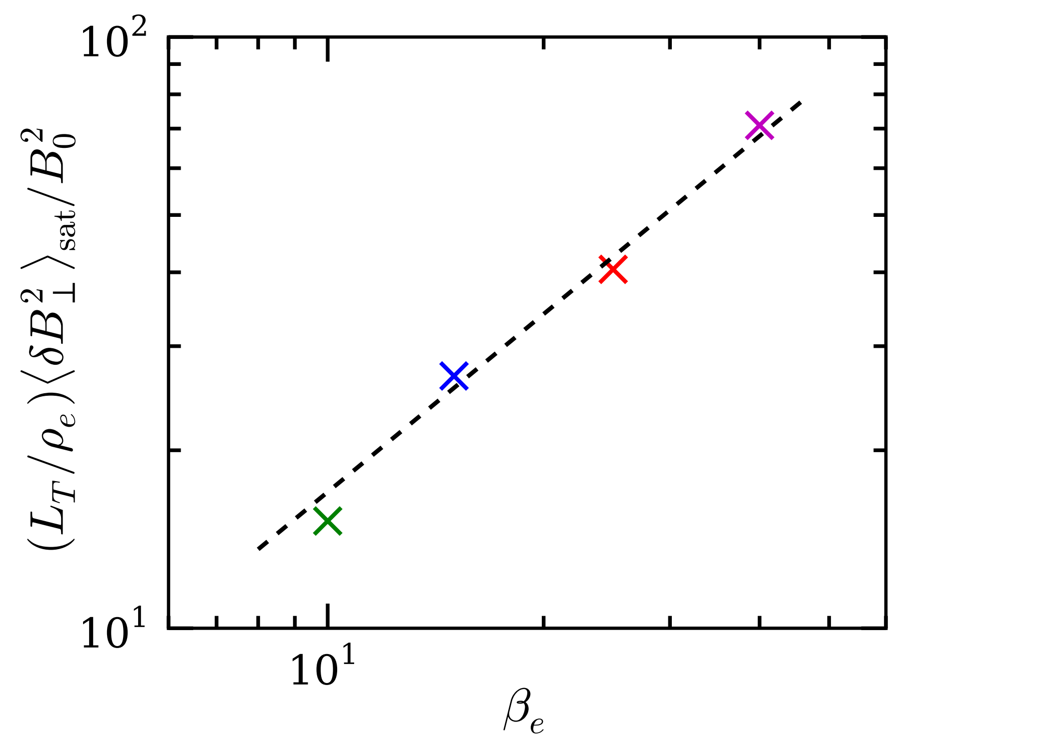

Relevance for galaxy clusters

modified Spitzer parallel heat flux (Coulomb collisions) :

$$q_{\parallel S} \approx 0.5 m_e n_e v_{th}^3 \frac{\lambda_e}{L_T + 4\lambda_e}$$

Heat flux regulated by instability:

$$q_{\parallel W} \approx 1.5 \beta_e^{-1} m_e n_e v_{th}^3 \frac{\lambda_e}{L_T + 4\lambda_e}$$

Suppression factor:

$$S_W \approx \frac{3}{\beta_e}\left(\frac{L_T}{\lambda_e} + 4\right)$$

$\beta_e = 100$, $\lambda_e = 20$ kpc -> $S_W^{min} \sim 1/10$; $S_W \sim 1/4$, $L_T = 100$ kpc

Heat flux and whistlers in solar wind

1. apparent beta-dependent limits on HF
2. mostly parallel whistlers
3. weak correlation between heat fluxes and whistler occurrence (selection effect?)
4. small amplitude (~0.01 B_0) consistent with QL estimate
5. strong effect of temperature anisotropy

Tong+ 2018

Tong+ 2019

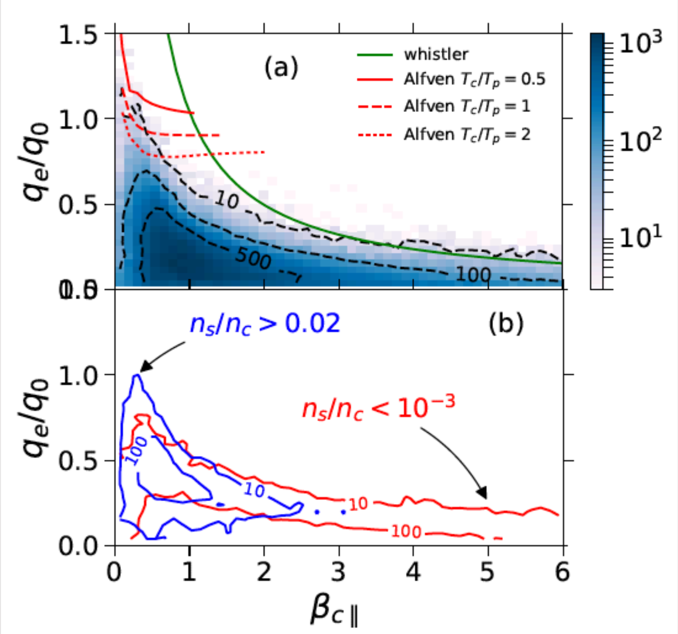

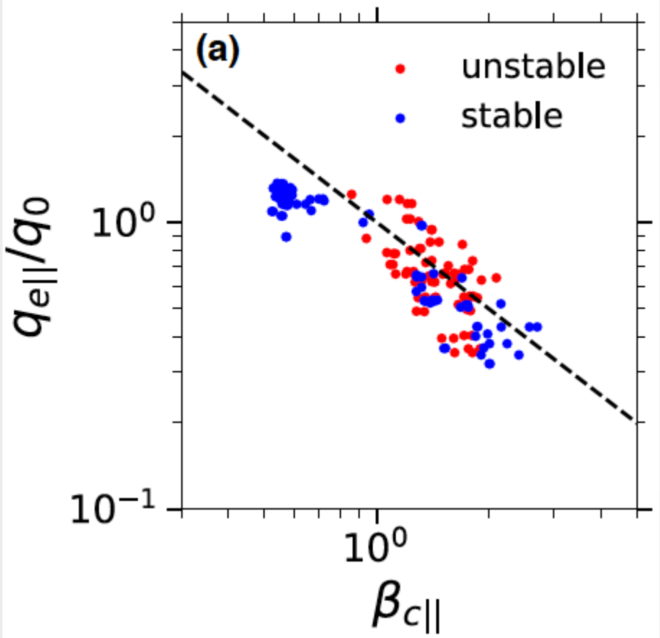

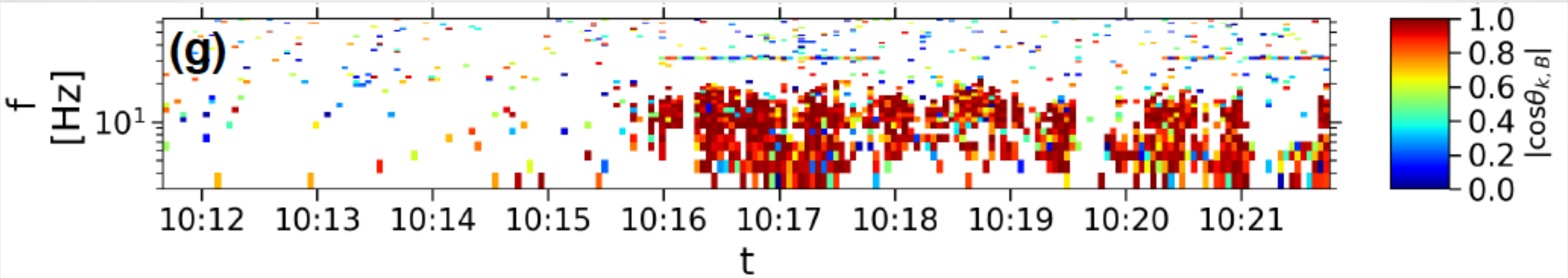

Heat flux and whistlers in solar wind

1. apparent beta-dependent limits on HF
2. mostly parallel whistlers
3. weak correlation between heat fluxes and whistler occurrence (selection effect?)
4. small amplitude (~0.01 B_0) consistent with QL estimate
5. strong effect of temperature anisotropy

Tong+ 2018
Tong+ 2019

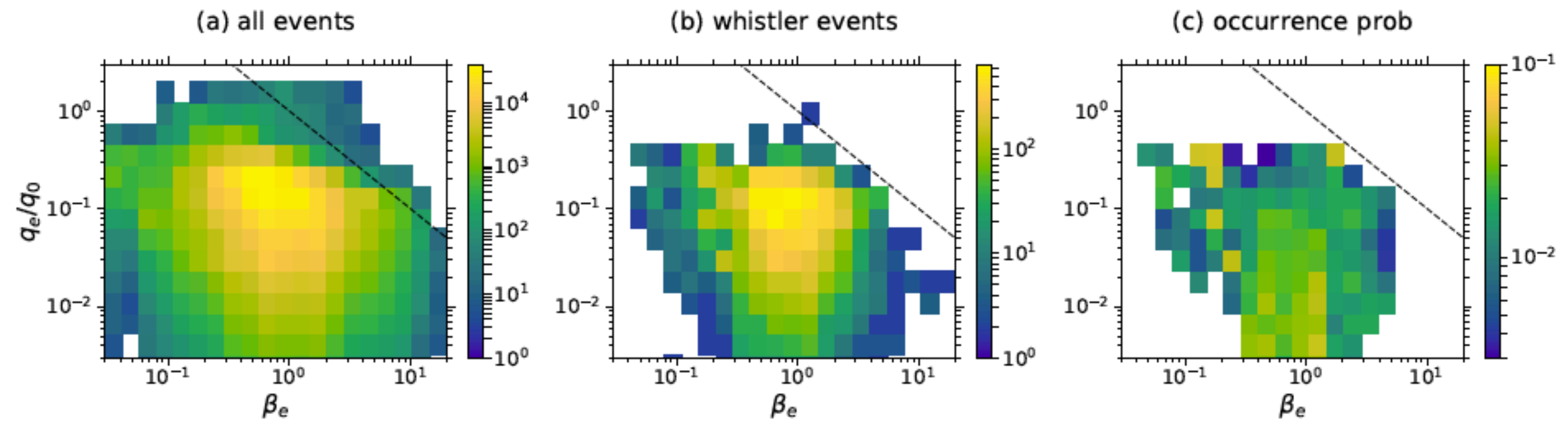

Heat flux and whistlers in solar wind

1. mostly parallel whistlers
2. weak correlation between heat fluxes and whistler occurrence (selection effect?)
3. small amplitude (~0.01 B_0) consistent with QL estimate

Tong+ 2018
Tong+ 2019

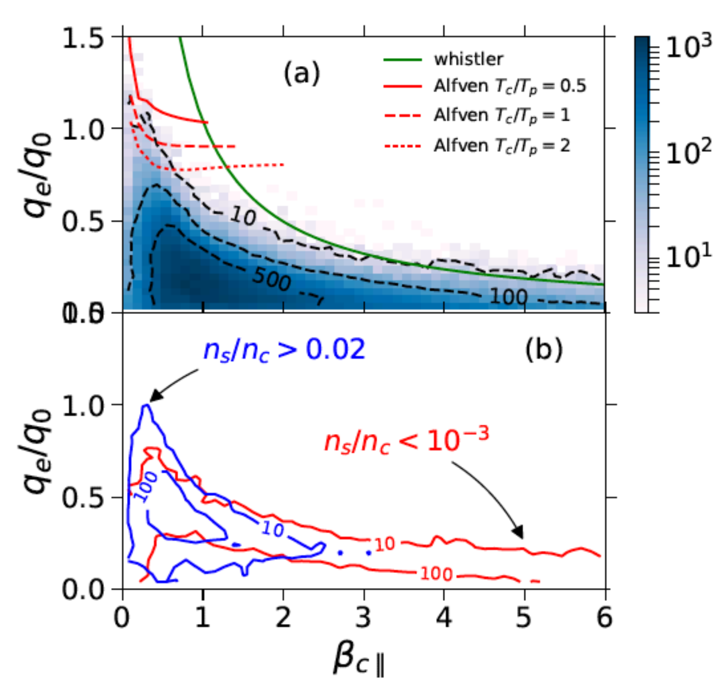

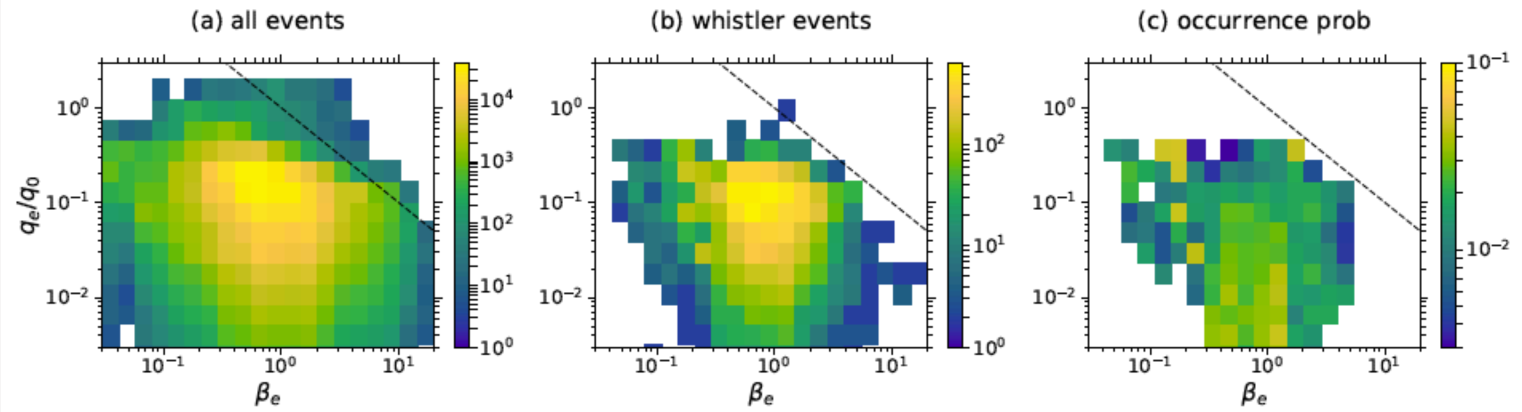

Summary

- Field-line draping likely explains survival of temperature fluctuations on scales ~10-100 kpc.
- Turbulence may enhance magnetic insulation locally or promote heat exchange at Pr~1.
- Mirror instability can produce suppression of parallel thermal conductivity ~1/5.
- Heat-flux induced whistlers may suppress heat fluxes at strong thermal gradients.